High gain observer for a class of nonlinear systems with coupled structure and sampled output measurements: application to a quadrotor

Omar Hernandez, Maria Eusebia Guerrero-Sánchez, M Farza, T Menard, Mohamed M'saad, Rogelio Lozano

High gain observer for a class of nonlinear systems with coupled structure and sampled output measurements: application to a quadrotor

Omar Hernández-González [a,b], María-Eusebia Guerrero-Sánchez [a,b], Mondher Farza[c], Tomas Ménard[c], Mohammed M'Saad[c] and Rogelio Lozano[a,d]

[a]Laboratorio Franco-Mexicano de Informática y Aeronáutica UMI-LAFMIA 3175 CNRS, CINVESTAV, Ciudad de México, México; [b]Tecnológico Nacional de México, Instituto Tecnológico Superior de Coatzacoalcos, Coatzacoalcos, Ver., México; [c]Normandie Université, UNICAEN, ENSICAEN, LAC EA 7478, Caen, France; [d]Sorbonne Universités, UTC CNRS UMR 7253 Heudiasyc, Compiègne, France

ABSTRACT

This paper proposes a new high gain observer for a class of non-uniformly observable nonlinear systems with coupled structure driven by sampled outputs. The considered class of systems is par-ticularly constituted by several subsystems where each subsystem is associated to a subset of the output variables. The observer design is carried out through two steps. First, a high-gain observer is proposed in the continuous-time output case under the assumption that an adequate persistent excitation condition is satisfied by each subsystem. Then, the proposed observer is redesigned to handle the case of sampled outputs leading thereby to a continuous-discrete time observer. The latter property is achieved thanks to the approach pursued along the convergence analysis. The effectiveness of the proposed observer is emphasised in a realistic simulation framework involving a mathematical model of a quadrotor which is diffeomorphic to the proposed class of considered systems.

1. Introduction

The observer design problem for nonlinear systems has been widely investigated over the last years, leading thereby to appropriate estimation algorithms that have been used in system control design as well as in fault detection and isolation that are commonly encountered in power systems. Several approaches have been proposed for the observer design of nonlinear systems, namely those based on canonical and normal observability forms. A well known contribution within this framework is the one proposed in Gauthier, Hammouri, and Othman (1992) where a necessary and sufficient condition for characterising the uniformly observable single output control affine systems. This canonical form is then used for the design of a high gain observer under some mild conditions as the global Lipschitz property of the nonlinearities. The gain of the proposed observer is derived from the resolution of an algebraic Lyapunov equation which expression has been given explicitly (see e.g. Besançon & Ticlea, 2007; Busawon, Farza, & Hammouri, 1998; Deza, Busvelle, & Gauthier, 1992; Dufour, Flila, & Hammouri, 2012; Farza, M'Saad, & Rossignol, 2004; Gauthier, 2001; Hammouri, Bornard, & Busawon, 2010; Hou, Busawon, & Saif, 2000).

The observer design problem for multi-output nonlinear systems that are observable for any input has been comprehensively investigated in Hammouri and Farza (2003) and Shim, Son, and Seo (2001) where several observability normal forms have been proposed according to the nature of the output decomposition. These contributions have been further alleviated, bearing in mind the observer design requirements, in Farza, Triki, M'Saad, and Maatoug (2011); Hammouri et al. (2010) where other observability normal forms for nonlinear uniformly observable systems have been proposed. In Hammouri et al. (2010), the observer design is carried out thanks to adequate sufficient conditions on the structure of the nonlinearities. This fundamental contribution has been further alleviated in Farza et al. (2011), where the observer design is naturally performed thanks to the structure of the involved normal from. On other aspects, a particular emphasis has been put on the challenging observer design problem for nonlinear systems that are not observable for any input thanks to specific

CONTACT María-Eusebia Guerrero-Sánchez maguerreros@itesco.edu.mx Laboratorio Franco-Mexicano de Informática y Aeronáutica UMI-LAFMIA 3175 CNRS, CINVESTAV, Ciudad de México, México Tecnológico Nacional de México, Instituto Tecnológico Superior de Coatzacoalcos, Carr. Anti. Mina-Coatza km. 16.5, Coatzacoalcos, Ver., México

persistent excitation conditions. These conditions characterise the input sequence for which the observability Gramian is positive definite on a sliding window with a fixed given width. This concept has been particularly used in Besançon and Ticlea (2007), where the class of locally regular inputs has been introduced to design high-gain observers for classes of state-affine systems assuming that the state-affine property depends on the inputs and outputs of the system. Nevertheless, there are two fundamental issues that have not been addressed yet, namely how to exhibit a canonical form for the whole set of nonlinear systems that observable for any input? and how to to characterise the class of persistently exciting input sequences for nonlinear systems that are not observable for any input?.

On other aspects, since the output measurements are generally transmitted through digital communication networks and are therefore available only at discrete-time instants t_κ, an important research activity has been devoted to the observer design problem for nonlinear systems with sampled output measurements (Dinh, Andrieu, Nadri, & Serres, 2015; Zhao & Hua, 2017; Zhao & Wang, 2014). Two approaches have been considered in these contributions. The first one is based on an exact or approximate discrete-time descriptions of the systems dynamics (Arcak & Nesic, 2004; Krener & Kravaris, 2001), while the second consists in a combination of a high gain observer together with an appropriate prediction between the sampling times (see for instance Deza, Busvelle, Gauthier, & Rakotopara, 1992; Hammouri, Nadri, & Mota, 2006; Karafyllis & Kravaris, 2009; Nadri, Hammouri, & Astorga, 2004). A comprehensive approach providing an appropriate reformulation of the continuous gain with a genuine adaptation to the sampling constraints has been proposed in Farza et al. (2014) and further alleviated in Farza, Bouraoui, Ménard, Abdennour, and M'Saad (2014) and Bouraoui et al. (2015) to handle the case of uncertain systems and simultaneous state and parameter estimation.

The observer design for quadrotors has been investigated in many works and has been the subject of active research and development for many years. The recent heavy application demands in quadrotors let to apply the robust control of UAVs through the use of high gain observers via output control. For instance: in Castillo et al. (2019) a disturbance observer-based quadrotor attitude controller is presented. The controller is capable to carry out precise and aggressive attitude maneuvers in the presence of high disturbances. The controller is made up of the cascade connection between two control-loops: an outer quaternion-based attitude control-loop and an inner disturbance observer-based angular velocity tracking control-loop. The disturbance observer is designed to estimate and compensate for the Coriolis term and the external disturbances. In Castañeda, Salas-Peña, and de Leon-Morales (2017) an attitude and airspeed controllers for a fixed wing unmanned aerial vehicle is designed. An adaptive super twisting controller for flight control of a fixed wing UAV under external disturbances is proposed for improving performance under different operating conditions and is robust in presence of external disturbances. Also, an extended state observer is used to estimate unmeasurable states of the system as well as external disturbances. In Rosaldo-Serrano, SantiaguilloSalinas, and Aranda-Bricaire (2019) an implementation of a time-varying version of the backstepping technique combined with suitable Luenberger observers to achieve trajectory tracking control for an UAV is presented. In Shao, Liu, and Wang (2018) a robust back-stepping output feedback trajectory tracking controller for quadrotors subject to parametric uncertainties and external disturbances is proposed. Also, a high-order ESO with special structure that relies only on position measurements is employed to estimate the unmeasurable states and the lumped disturbances in rotational subsystem simultaneously. In Wang, Yu, Mu, and Zhang (2019) a disturbance observer-based adaptive sliding mode control strategy for a quadrotor helicopter subject to multiple actuator faults, parametric uncertainties, and external disturbances is presented.

The aim of this paper is to extend the high gain observer design proposed in Farza et al. (2011) for uniformly observable nonlinear systems with coupled structure to a class of multi-output non-uniformly observable systems with sampled output measurements. More specifically, the involved class of systems is composed by several non-uniformly observable subsystems where each subsystem is associated to all or a part of the output components, allowing thereby each subsystem dynamics to depend on every state variable of the system. Two design features are worth to be pointed out:

- Firstly, an observer is designed by assuming that the outputs are available in a continuous manner. The underlying observer gain associated to each subsystem is determined through the resolution of an appropriate Lyapunov Ordinary Differential Equation (ODE) involving a single design parameter up to a suitable persistent excitation condition. Such a feature allows to handle the high gain observer design for nonlinear systems that are not necessarily uniformly observable and the overall system does not assume a triangular structure, unlike in previous works (Farza et al., 2011; Hernández-González et al., 2016), which only addresses to uniformly observable systems and assumes a triangular structure for each subsystem, respectively.

- Secondly, the provided observer is redesigned in order to account for the sampling process of the outputs. The approach pursued through the redesign borrows from the one proposed in Farza et al. (2014). Of fundamental interest,the convergence of the proposed observer is established throughout a comprehensive convergence analysis approach allowing a reasonable sampling process for the output measurements, namely the maximum value of the sampling partition diameter is lower than a certain given bound. This continuous-discrete observer will in turn serve to propose new continuous control schemes where required of large sampling rates, this necessarily implies of the sensors and controllers more expensive.

In addition, the control designs for the quadrotor have presented some of the following restrictions with respect to the proposed observer in this work:

- The existing observer design results present complexity in its calibration. The proposed algorithm is a continuous-discrete time observer for a quadrotor with simplicity in its calibration, which through the choice of a single real positive design parameter is achieved.
- Problems in the exponential convergence of the state error to zero for reasonably long sampling periods, since the output measurements are generally available only at discrete-time instants. The proposed observer works for relatively large sampling times. This is a main contribution because the existing observer design results fail to provide a good behaviour when the sample time is large.

Motivated by the aforementioned considerations, in this paper, we offer an alternative approach helps to improve the performance of the system.

The paper is organised as follows. The observer design problem statement is presented in Section 2 with a particular emphasis on the involved modeling and design assumptions for the underlying continuous time observer design. The latter is provided in Section 3 with its pertinent properties. Section 4 is devoted to the main contribution of the paper, namely the proposed observer for the considered class of nonlinear systems with sampled output measurements together with the fundamental result on its convergence property. Simulation results involving a realistic physical model of an unmanned aerial vehicle are given in Section 5 to show the performance of the proposed observer. Section 6 overviews the motivation of the paper with a particular emphasis on the interest of its fundamental result.

Throughout the paper, for any positive integer k, I_k and 0_k denote the k-dimensional identity and null matrices respectively, $\|.\|$ denotes the euclidian norm and for any Symmetric Definite Positive time varying matrix $Q(t)$, $\lambda_m(Q(t))$ (respectively $\lambda_M(Q(t))$) will be used to denote the smallest (respectively the largest) eigenvalue of $Q(t)$ and $\underline{\lambda}_m(Q) = \inf_{t\geq t_o} \lambda_m(Q(t))$, $\overline{\lambda}_M(Q) = \sup_{t\geq t_o} \lambda_M(Q(t))$ where t_o is any fixed non-negative time instant. Furthermore, the function arguments will be omitted when clear from the context.

2. Problem statement

One aims at alleviating the available high gain observer design contributions by further enlarging the involved class of systems. More specifically, one shall consider the following class of multivariable state affine nonlinear systems

$$\mathcal{SYS}\begin{cases}\dot{x}(t) = A\left(u(t)\right)x(t) + \varphi\left(u(t), x(t)\right)\\ y(t_k) = Cx\left(t_k\right)\end{cases} \tag{1}$$

$x(t) \in \mathbb{R}^n$, $u(t) \in \mathbb{R}^m$ and $y(t) \in \mathbb{R}^p$ denote, respectively, the state, the input and the output of the system that are particularly partitioned as follows

$$x(t) = \begin{bmatrix} x^1 \\ x^\kappa \\ x^q \end{bmatrix} \in \mathbb{R}^n \quad \text{with} \quad x^\kappa = \begin{bmatrix} x_1^\kappa \\ x_i^\kappa \\ x_{\lambda_\kappa}^\kappa \end{bmatrix} \in \mathbb{R}^{n_\kappa},$$

$$x_i^\kappa = \begin{bmatrix} x_{i,1}^\kappa \\ x_{i,j}^\kappa \\ x_{i,p_\kappa}^\kappa \end{bmatrix} \in \mathbb{R}^{p_\kappa} \quad \text{and} \quad x_{i,j}^\kappa \in \mathbb{R},$$

$y(t) = [\, {}^{cy_1}\, y_\kappa\, y_q\,]^{\mathrm{T}} \in \mathbb{R}^p$ with $y_\kappa \in \mathbb{R}^{p_\kappa}$, and $p_\kappa \geq 1$, $\lambda_\kappa \geq 2$, $\sum_{\kappa=1}^q n_\kappa = \sum_{\kappa=1}^q p_\kappa \lambda_k = n$ with $\sum_{\kappa=1}^q p_\kappa = p$.

The system output is only available at the sampling times $0 \leq t_o < \cdots < t_k < t_{k+1} < \cdots$ with $\lim_{k\to\infty} t_k = +\infty$, where $\tau_k = t_{k+1} - t_k$ are time-varying intervals such that there exists $\tau_{\max} > 0$ such that $0 < \tau_k \leq \tau_{\max}$ $\forall k \geq 0$. The matrices $A(u)$ and C are respectively given by

$$A(u) = \begin{bmatrix} A_1(u) & 0 & \cdots & 0 \\ 0 & \ddots & \ddots & 0 \\ \vdots & \ddots & \ddots & 0 \\ 0 & 0 & 0 & A_q(u) \end{bmatrix} \text{ with}$$

$$A_\kappa(u) = \begin{bmatrix} 0 & A_{\kappa,1}(u) & 0 & 0 \\ \vdots & \ddots & \ddots & 0 \\ 0 & & \ddots & A_{\kappa,\lambda_\kappa-1}(u) \\ 0 & 0 & 0 & 0 \end{bmatrix},$$

and

$$C = \begin{bmatrix} C_1 & 0 & 0 \\ 0 & \ddots & 0 \\ 0 & 0 & C_q \end{bmatrix} \text{ with } C_\kappa = \begin{bmatrix} I_{p_\kappa} & 0 & \cdots & 0 \end{bmatrix},$$

where the functions $A_{\kappa,i}$ for $\kappa = 1,\ldots,q$ and $i = 1,\ldots,\lambda_\kappa - 1$ are continuous with respect to u. And $\varphi : \mathbb{R}^n \times \mathbb{R}^m \mapsto \mathbb{R}^n$ is a nonlinear function given by

$$\varphi(u,x) = \begin{bmatrix} \varphi^1(u,x) & \varphi^2(u,x) & \ldots & \varphi^q(u,x) \end{bmatrix}^T \in \mathbb{R}^n$$

with

$$\varphi^\kappa(u,x) = \begin{bmatrix} \varphi_1^\kappa(u,x) & \varphi_2^\kappa(u,x) & \ldots & \varphi_{\lambda_\kappa}^\kappa(u,x) \end{bmatrix}^T \in \mathbb{R}^{n_\kappa}, \tag{2}$$

where $\varphi_i^\kappa : \mathbb{R}^n \times \mathbb{R}^n \mapsto \mathbb{R}^{p_\kappa}$ is differentiable w.r.t. x for $\kappa = 1,\ldots,q$ and $i = 1,\ldots,\lambda_\kappa$, measurable with respect to u and assumes the following structural dependence on the state variables for $\kappa = 1,\ldots,q$ and $i = 1,\ldots\lambda_\kappa - 1$

$$\varphi_i^\kappa(u,x) = \varphi_i^\kappa(u,x^1,x^2,\ldots,x^{\kappa-1}, x_1^\kappa,x_2^\kappa,\ldots,x_i^\kappa,x_1^{\kappa+1},x_1^{\kappa+2},\ldots,x_1^q) \tag{3}$$

$$\varphi_{\lambda_\kappa}^\kappa(u,x) = \varphi_{\lambda_\kappa}^\kappa(u,x^1,x^2,\ldots,x^q). \tag{4}$$

More specifically, the high gain observer design is well posed provided that the following usual assumptions are satisfied (see for instance Besançon, Bornard, & Hammouri, 1996; Farza et al., 2011)

A1 The state $x(t)$ and the control $u(t)$ are bounded, i.e. $x(t) \in X$ and $u(t) \in U$ where $X \subset \mathbb{R}^n$ and $U \subset \mathbb{R}^m$ are compact sets.

A2 The function $\varphi(.,.)$ is Lipschitz w.r.t. $x \in X$ uniformly w.r.t. $u \in U$.

According to **A1**, the matrices $A_\kappa(u(t))$ and $A(u(t))$ are upper bounded, i.e. there exists positive scalars $\bar{a}_\kappa$ and $\bar{a}$ such that

$$\bar{a}_\kappa = \sup_{t\geq 0} \|A_\kappa(u(t))\| \quad \text{and} \quad \bar{a} = \sup_{t\geq 0} \|A(u(t))\|. \tag{5}$$

Remark 2.1: There are three features that have to be pointed out to appreciate how large is the considered class of systems with respect to the open literature. Firstly, the coupling structure (3)–(4) is borrowed from the available results on the high gain observer design for uniformly observable nonlinear systems (Farza et al., 2011; Shim et al., 2001). Recall that the main motivation of these contributions was to circumvent the triangular structure since the problem of sampled output measurements was not considered. Secondly, the extension from uniformly observable systems to non-uniformly observable systems is carried out thanks to the comprehensive high gain observer design approaches proposed in Besançon et al. (1996) and Hammouri and Farza (2003) for triangular systems assuming that the output measurements are continuously available. Such an extension is feasible thanks to an appropriate persistent excitation condition on the input sequence which will be naturally stated in the following section. Thirdly, the problem of sampled output measurements is addressed in the high gain observer design framework provided in Farza et al. (2014).

Remark 2.2: It is worth noting that the state x_i^κ can be further decomposed, since, the output of each block may be a vector and is not necessary a single signal. In order to illustrate this issue, the following example is given: consider the state vector $x = [x^1 \quad x^2]^{\mathrm{T}}$, where the first system is constituted as follows $x^1 = \begin{bmatrix} x_1^1 & x_2^1 & x_3^1 \end{bmatrix}^{\mathrm{T}}$, $x_1^1 = \begin{bmatrix} x_{1,1}^1 = x_1 \\ x_{1,2}^1 = x_2 \end{bmatrix}$, $x_2^1 = \begin{bmatrix} x_{2,1}^1 = x_3 \\ x_{2,2}^1 = x_4 \end{bmatrix}$, $x_3^1 = \begin{bmatrix} x_{3,1}^1 = x_5 \\ x_{3,2}^1 = x_6 \end{bmatrix}$; and the second system is constituted as follows $x^2 = \begin{bmatrix} x_1^2 = x_7 \\ x_2^2 = x_8 \end{bmatrix}$; finally, the following overall output is expressed as $y = [\bar{y}_1 \ \bar{y}_2]^{\mathrm{T}}$, where $\bar{y}_1 = x_1^1 = \begin{bmatrix} y_1 = x_1 \\ y_2 = x_2 \end{bmatrix}$ and $\bar{y}_2 = x_1^2 = [y_3 = x_7]$. Thus, this notation is in the form (1) with $q = 2$, $p_1 = 2$ and $p_2 = 1$.

For clarity purposes, let us introduce a specific matrix for high gain observer design together with technical results that will be used throughout the observer convergence analysis. The involved matrix is given by

$$\Delta_\kappa(\theta) = \mathrm{diag}\begin{bmatrix} I_{p_\kappa} & \theta^{-\delta_\kappa} I_{p_\kappa} & \ldots & \theta^{-\delta_\kappa(\lambda_\kappa-1)} I_{p_\kappa} \end{bmatrix}, \tag{6}$$

where $\theta \geq 1$ is a real number and the powers δ_κ are determined as follows

$$\delta_\kappa = 2^{q-\kappa}\left(\prod_{i=\kappa+1}^{q}\left(\lambda_i - \frac{3}{2}\right)\right) \text{ for} \kappa = 1,\ldots,q-1,$$
$$\delta_q = 1. \tag{7}$$

Then, one has

$$\frac{\delta_\kappa}{2} = \left(\lambda_{\kappa+1} - \frac{3}{2}\right)\delta_{\kappa+1} \text{ for } \kappa = 1, \ldots, q-1. \quad (8)$$

Note that since $\lambda_\kappa \geq 2$, one has $(\lambda_{\kappa+1} - \frac{3}{2}) \geq \frac{1}{2}$ and therefore $\{\delta_\kappa\}_{1\leq\kappa\leq q}$ constitutes a non-increasing sequence of positive real numbers, i.e.

$$\delta_1 \geq \delta_2 \geq \cdots \geq \delta_q = 1. \quad (9)$$

Now, one shall recall a technical lemma given in Farza et al. (2011) which provide a sequence of reals that reflects in some sense the interconnections between the subsystems nonlinearities. The sequence $\{\delta_\kappa\}$ is related to the interconnections between the subsystem nonlinearities.

Lemma 2.1 (Farza et al., 2011): *Let*

$$\chi_{l,j}^{\kappa,i} = \begin{cases} 0 & \text{if } \dfrac{\partial \varphi_i^\kappa}{\partial x_j^l}(u,x) \equiv 0, \\ 1 & \text{otherwise,} \end{cases} \quad (10)$$

for $\kappa, l = 1, \ldots, q$, $i = 1, \ldots, \lambda_\kappa$ *and* $j = 2, \ldots, \lambda_l$, *and consider the sequence of real numbers*

$$\sigma_i^\kappa = \sigma_1^\kappa + (i-1)\delta_\kappa, \quad (11)$$

with

$$\sigma_1^\kappa = -(\lambda_\kappa - 1)\delta_\kappa + (\lambda_1 - 1)\delta_1 + \eta\left(1 - \frac{1}{2^{\kappa-1}}\right), \quad (12)$$

where $0 < \eta \leq 1$ *can be chosen arbitrarily small, and the sequence* $\{\delta_\kappa\}_{1\leq\kappa\leq q}$ *are given by* (9). *Then, one has*

$$\text{if } \chi_{l,j}^{\kappa,i} = 1 \text{ then } \sigma_j^l - \sigma_i^\kappa - \frac{\delta_l}{2} - \frac{\delta_\kappa}{2} \leq -\frac{\eta}{2^q}. \quad (13)$$

Note that it has been shown in Farza et al. (2011) that $\sigma_i^\kappa \leq 0$, for $\kappa = 1, \ldots, q$ and $i = 1, \ldots, \lambda_\kappa$. Now, similarly to the matrices $\Delta_\kappa(\theta)$, one defines the diagonal matrices Λ_κ as follows

$$\Lambda_\kappa(\theta) = \theta^{-\sigma_1^\kappa}\Delta_\kappa(\theta) \text{ for } \kappa = 1, \ldots, q. \quad (14)$$

Taking into account the structures of $\Lambda_\kappa(\theta)$, $\Delta_\kappa(\theta)$, A_κ and C_κ, one can easily check the following equalities

$$\begin{aligned} \Lambda_\kappa(\theta)A_\kappa(u)\Lambda_\kappa^{-1}(\theta) &= \Delta_\kappa(\theta)A_\kappa(u)\Delta_\kappa^{-1}(\theta) \\ &= \theta^{\delta_\kappa}A_\kappa(u), \end{aligned} \quad (15)$$

$$\theta^{-\sigma_1^\kappa}C_\kappa\Lambda_\kappa^{-1}(\theta) = C_\kappa\Delta_\kappa^{-1} = C_\kappa. \quad (16)$$

Now, one needs the following technical result when investigating the problem of continuous-time estimation of the state from sampled outputs. Such a result has been established in Bouraoui et al. (2015).

Lemma 2.2: *Consider a differentiable function* $v : t \in \mathbb{R}^+ \mapsto v(t) \in \mathbb{R}^+$ *satisfying the following inequality*

$$\begin{aligned} \dot{v}(t) &= -av(t) + b\int_{t_\kappa}^{t} v(s)\,\mathrm{d}s \\ &\forall t \in [t_k, t_{k+1}[\quad \text{with} \quad k \in \mathbb{N}, \end{aligned} \quad (17)$$

where $0 < t_{k+1} - t_k \leq \tau_{\max}$, *thus a and b are positive reals satisfying*

$$\frac{b}{a}\tau_{\max} < 1. \quad (18)$$

Then, the function v converges exponentially to zero, i.e.

$$\begin{aligned} v(t) &\leq e^{-\eta(t-t_o)}v(t_o) \quad \text{with} \\ 0 &< \eta = (a - b\tau_{\max})\,e^{-a\tau_{\max}}. \end{aligned} \quad (19)$$

In the following section, one shall design a high gain observer for the class of systems (1) in the case where the output measurements are continuously available. Then, the underlying observer shall be appropriately redesigned in order to account for the output sampling process.

3. The underlying continuous-time observer

Let us first point out that the κ-th block, $\kappa = 1, \ldots, q$, of system (1) can be expressed as follows

$$\begin{aligned} \dot{x}^\kappa(t) &= A_\kappa\left(u(t)\right)x^\kappa(t) + \varphi^\kappa\left(u(t), x(t)\right) \\ y_k(t) &= C_\kappa x^\kappa(t). \end{aligned} \quad (20)$$

Bearing in mind the available results on the high gain observer design, the following dynamical system would be a suitable candidate observer.

$$\begin{aligned} \dot{\hat{x}}^\kappa(t) &= A_\kappa(u(t))\hat{x}^\kappa(t) + \varphi^\kappa(u(t), \underline{\hat{x}}(t)) \\ &\quad - \theta^{\sigma_\kappa}\Delta_\kappa(\theta)^{-1}S_\kappa^{-1}(t)C_\kappa^{\mathrm{T}}\left(C_\kappa\hat{x}^\kappa(t) - y_\kappa(t)\right) \\ \dot{S}_\kappa(t) &= \theta^{\delta_\kappa}\Big(-S_\kappa(t) - A_\kappa(u(t))^{\mathrm{T}}S_\kappa(t) \\ &\quad - S_\kappa(t)A_\kappa(u(t)) + C_\kappa^{\mathrm{T}}C_\kappa\Big), \end{aligned} \quad (21)$$

where $u(t) \in \mathbb{R}^m$ and $y(t) \in \mathbb{R}^p$ are, respectively, the input and the output of system (1), the matrix $\Delta_\kappa(\theta)$ is given by (7), $S_\kappa(0) = S_\kappa^{\mathrm{T}}(0) > 0$, $\theta \geq 1$ is a scalar design parameter; $\hat{x} \in I\!R^n$ denotes the state estimate given by $\hat{x} = (\hat{x}^1 \ \ldots \ \hat{x}^q)^{\mathrm{T}} \in I\!R^n$ with $\hat{x}^\kappa = (\hat{x}_1^\kappa \ \ldots \ \hat{x}_1^\kappa)^{\mathrm{T}} \in I\!R^{p_\kappa}$, $\underline{\hat{x}}^\kappa$ denotes a state estimate up to an output injection, i.e.

$$\underline{\hat{x}}_i^\kappa = \begin{cases} x_1^\kappa & \text{for} \quad i = 1, \\ \hat{x}_i^\kappa & \text{for} \quad i = 2, \ldots, \lambda_\kappa. \end{cases}$$

Now, one assumes the following additional assumption

A3 The input sequence $u(t)$ is persistently exciting, i.e. satisfies the following property $\exists \theta^* > 0$, $\exists \delta_o > 0$ and $\forall \theta \geq \theta^*$, one has

$$\int_{t-1/\theta^{\delta_\kappa}}^{t} \left(\Phi_u^\kappa(s,t)\right)^T C_\kappa^T C_\kappa \Phi_u^\kappa(s,t)\, \mathrm{d}s \geq \frac{\delta_o}{\theta^{\delta_\kappa}\alpha(\theta)} \Delta_\kappa^2(\theta), \quad \forall\, \kappa, \geq \frac{1}{\theta^{\delta_\kappa}}, \tag{22}$$

where $\alpha(\theta) \geq 1$ is a function satisfying

$$\lim_{\theta\to\infty} \frac{\alpha(\theta)}{\theta^{\frac{\eta}{2^{q-1}}}} = 0, \tag{23}$$

and where $\Phi_u^\kappa(t,s)$ denotes the state transition matrix of the state affine system

$$\dot{\xi}_\kappa(t) = A_\kappa(u(t))\xi_\kappa(t). \tag{24}$$

Recall that $\Phi_u^\kappa(t,s)$ as follows

$$\dot{\Phi}_u^\kappa(t,s) = A_\kappa(u(t))\Phi_u^\kappa(t,s)\ \forall t \geq s \geq 0 \quad \text{with} \quad \Phi_u^\kappa(t,t) = I_{n_\kappa}\ \forall t \geq 0. \tag{25}$$

Note that Assumption **A3**, which is similar to that considered in Dufour et al. (2012), is of primary importance for the stability of the observer. Indeed, this assumption is satisfied for uniformly observable systems, i.e. systems which are observable for any input. For non-uniformly observable systems, the characterisation of the class of inputs which satisfy Assumption **A3** is still an open problem. Indeed, the authors in Besançon and Ticlea (2007) and Dufour et al. (2012), respectively, introduced the notion of local regular inputs and regular inputs. Assumption **A3** extends the definition of regular inputs given in Dufour et al. (2012) to the class of cascaded systems (1). One now states the following.

Theorem 3.1: *Consider system* (1) *subject to assumptions* **A1** *and* **A2**. *Then, for every bounded input satisfying assumption* **A3**, *there exists a constant* θ^* *such that for every* $\theta > \theta^*$, *the system* (21) *is a state observer for system* (1) *with an exponential error convergence to the origin for sufficiently high values of* θ, *namely for any initial conditions* $(x(0), \hat{x}(0)) \in X \times X$, *the observation error* $\hat{x}(t) - x(t)$ *converges exponentially to zero.*

Proof of Theorem 3.1: Let us first derive a lower bound for the smallest eigenvalue of each SPD matrix $S_\kappa(t)$ appearing in the observer (21). This property can be easily established by remarking that the transition matrix of the following state affine system

$$\dot{\xi}_\kappa = \theta^{\delta_\kappa} A_\kappa(u)\xi_\kappa, \tag{26}$$

is given by

$$\tilde{\Phi}_u^\kappa = \Delta_\kappa(\theta)\Phi_u^\kappa(t,s)\Delta_\kappa(\theta)^{-1}, \tag{27}$$

where Φ_u^κ is the transition matrix defined by Equation (25). Indeed, the matrix $S_\kappa(t)$ can be expressed as

$$S_\kappa(t) = e^{-\theta^{\delta_\kappa} t}(\tilde{\Phi}_u^\kappa)^{\mathrm{T}}(0,t)S_\kappa(0)\tilde{\Phi}_u^\kappa(0,t) + \theta^{\delta_\kappa}\int_o^t e^{-\theta^{\delta_\kappa}(t-s)}(\tilde{\Phi}_u^\kappa)^{\mathrm{T}}(s,t)C_\kappa^{\mathrm{T}}C_\kappa\tilde{\Phi}_u^\kappa(s,t)\,\mathrm{d}s. \tag{28}$$

Taking into account the second identity in (16), i.e. $C_\kappa\Delta_\kappa(\theta) = C_\kappa$, and the fact that $S_\kappa(0) = S_\kappa^{\mathrm{T}}(0) > 0$, one gets

$$S_\kappa(t) \geq \theta^{\delta_\kappa}\int_o^t e^{-\theta^{\delta_\kappa}(t-s)}\Delta_\kappa(\theta)^{-1}(\Phi_u^\kappa)^{\mathrm{T}}(s,t) \times C_\kappa^{\mathrm{T}}C_\kappa\Phi_u^\kappa(s,t)\Delta_\kappa(\theta)^{-1}\,\mathrm{d}s \geq e^{-1}\frac{\delta t_o}{\alpha(\theta)}I_{n_\kappa}, \tag{29}$$

where δ_o and $\alpha(\theta)$ are given by assumption **A3**. One can hence easily conclude that

$$\underline{\lambda}_m(S_\kappa) \geq \frac{e^{-1}\delta_o}{\alpha(\theta)}. \tag{30}$$

Let us now show that greater eigenvalue of each SPD matrix S_κ, i.e. $\overline{\lambda}_M(S_\kappa)$, is bounded with an upper bound independent of θ. To this end, one shall show that this property is satisfied for each (block) entry $(S_\kappa)_{i,j}$ of the matrix S_κ. According to the first equation of (21), one has

$$(\dot{S}_\kappa)_{1,1} = -\theta^{\delta_\kappa}((S_\kappa)_{1,1} - I_{p_\kappa}) \tag{31}$$

$$(\dot{S}_\kappa)_{1,j} = -\theta^{\delta_\kappa}((S_\kappa)_{1,j} + (S_\kappa)_{1,j-1}(t)A_{\kappa,\,j-1}(u))\ \text{for}\ j = 2,\ldots,n \tag{32}$$

$$(\dot{S}_\kappa)_{i,j} = -\theta^{\delta_\kappa}((S_\kappa)_{i,j} + (S_\kappa)_{i,j-1}(t)A_{\kappa,\,j-1}(u) + A_{\kappa,\,i-1}^{\mathrm{T}}(u)(S_\kappa)_{i-1,j}) \quad \text{for}\ i = 2,\ldots,n, j = i,\ldots,n. \tag{33}$$

It is clear from Equation (31) that

$$\left\|(S_k)_{1,1}(t)\right\| \leq \left\|(S_k)_{1,1}(0)\right\| + 1.$$

and for $j \geq 2$, one can proceed by induction in order to show that $(S_\kappa)_{1,j}$ is bounded with a bound independent

of θ. Indeed, assume that $(S_k)_{1,j-1}$ is bounded and set

$$S_M = \sup_{t\geq 0} \left\| (S_k)_{1,j-1} \right\|. \tag{34}$$

Taking into account (32), one gets

$$\begin{aligned}
&\|(S_\kappa)_{1,j}(t)\| \\
&\quad \leq e^{-\theta t}\|(S_\kappa)_{1,j}(0)\| \\
&\qquad + \theta \int_0^t e^{-\theta(t-s)} \|(S_\kappa)_{1,j-1}(s) A_{\kappa,j-1}(u(s))\| \, \mathrm{d}s \\
&\quad \leq \|(S_\kappa)_{1,j}(0)\| + \theta S_M \tilde{a}_\kappa \int_0^t e^{-\theta(t-s)} \, \mathrm{d}s \\
&\quad \leq \|(S_\kappa)_{1,j}(0)\| + S_M \tilde{a}_\kappa,
\end{aligned}$$

where $\tilde{a}_\kappa$ is the upper bound of $\|\tilde{A}_\kappa\|$. And using a similar induction procedure, one can show that every entries of $\|S_\kappa(t)\|$ are upper bounded independently of θ. In the following, one shall prove the exponential convergence to zero of the κ^{th} subcomponent of the observation error, i.e. $\tilde{e}(t) = \hat{x}(t) - x(t) \in \mathbb{R}^{n_\kappa}$. One has

$$\dot{\tilde{e}}^\kappa = \left(A_\kappa(u) - \theta^{\delta_\kappa} \Delta_\kappa^{-1}(\theta) S_\kappa^{-1} C_\kappa^{\mathrm{T}} C_\kappa \right) \tilde{e}^\kappa + \tilde{\varphi}^\kappa(u, \underline{\hat{x}}, x), \tag{35}$$

with $\tilde{\varphi}^\kappa(u, \underline{\hat{x}}, x) = \varphi^\kappa(u, \underline{\hat{x}}) - \varphi(u, x)$, and set

$$\bar{e}^\kappa(t) = \Lambda_\kappa(\theta) \tilde{e}^\kappa(t) \quad \text{for } \kappa = 1, \ldots, q, \tag{36}$$

where $\Lambda_\kappa(\theta)$ is given by (14). Using Equations (16) and (36), Equation (35) becomes

$$\dot{\bar{e}}^\kappa = \theta^{\delta_\kappa} A_\kappa(u) - S_\kappa^{-1} C_\kappa C_\kappa \bar{e}^\kappa + \Lambda_\kappa(\theta) \tilde{\varphi}^\kappa\left(u, \underline{\hat{x}}, x\right). \tag{37}$$

This makes it possible to show the exponential convergence to zero of the estimation error using an adequate approach based on the following Lyapunov candidate function

$$V(\bar{e}(t)) = \bar{e}^T(t) S(t) \bar{e}(t), \tag{38}$$

with $S(t) = \mathrm{diag}[\, S_1(t) \cdots S_\kappa(t) \cdots S_q(t) \,]$. Indeed, one has

$$V_\kappa\left(\bar{e}^\kappa\right) = \sum_{i=1}^{q} \left(\bar{e}^\kappa\right)^T S_\kappa \bar{e}^\kappa, \tag{39}$$

where S_κ is given by (21). Differentiating $V_\kappa(\bar{e}^\kappa)$ along the trajectories of system (37) yields

$$\dot{V}_\kappa\left(\bar{e}^\kappa\right) = 2\left(\bar{e}^\kappa\right)^{\mathrm{T}} S_\kappa \dot{\bar{e}}^\kappa + \left(\bar{e}^\kappa\right)^{\mathrm{T}} \dot{S}_\kappa \bar{e}^\kappa. \tag{40}$$

Combining (21) and (37) with (40) yields

$$\begin{aligned}
\dot{V}_\kappa\left(\bar{e}^\kappa\right) &= -\theta^{\delta_\kappa} \bar{e}^\kappa S_\kappa \bar{e}^\kappa - \theta^{\delta_\kappa} \bar{e}^\kappa C_\kappa^T C_\kappa \bar{e}^\kappa \\
&\quad + 2\left(\bar{e}^\kappa\right)^{\mathrm{T}} S_\kappa \Lambda_\kappa(\theta) \tilde{\varphi}^\kappa\left(u, \underline{\hat{x}}, x\right) \\
&\leq -\theta^{\delta_\kappa} \left(\bar{e}^\kappa\right)^{\mathrm{T}} S_\kappa \bar{e}^\kappa + 2\sqrt{\overline{\lambda}_M(S_\kappa)} \sqrt{V_\kappa}\left(\bar{e}^\kappa\right) \\
&\quad \times \sum_{i=1}^{\lambda_\kappa} \frac{1}{\theta^{\sigma_i^\kappa}} \left\| \tilde{\varphi}_i^\kappa\left(u, \underline{\hat{x}}, x\right) \right\|,
\end{aligned} \tag{41}$$

where $\sigma_i^\kappa = \sigma_1^\kappa + (i-1)\delta_\kappa$. And taking into account assumptions **A1–A2**, one has

$$\begin{aligned}
\dot{V}_\kappa\left(\bar{e}^\kappa\right) &\leq -\theta^{\delta_\kappa} V_\kappa\left(\bar{e}^\kappa\right) + 2L_{\tilde{\varphi}^\kappa} \sqrt{\overline{\lambda}_M(S_\kappa)} \sqrt{V_\kappa\left(\bar{e}^\kappa\right)} \\
&\quad \times \sum_{i=1}^{\lambda_\kappa} \sum_{l=1}^{q} \sum_{j=2}^{\lambda_l} \chi_{l,j}^{k,i} \theta^{-\sigma_i^\kappa} \left\| \bar{e}_j^l \right\|,
\end{aligned} \tag{42}$$

where $L_{\tilde{\varphi}^\kappa}$ denotes the Lipschitz constant of the function $\tilde{\varphi}^\kappa$, which exists according to assumption **A2**, and the $\chi_{l,j}^{\kappa,i}$ are defined as in Lemma 2.1. Moreover, one can rewrite (42) as follows

$$\begin{aligned}
\dot{V}_\kappa\left(\bar{e}^\kappa\right) &\leq -\theta^{\delta_\kappa} V_\kappa\left(\bar{e}^\kappa\right) + 2L_{\tilde{\varphi}^\kappa} \sqrt{\overline{\lambda_M}(S_\kappa)} \sqrt{V_\kappa\left(\bar{e}^\kappa\right)} \\
&\quad \times \sum_{i=1}^{\lambda_\kappa} \sum_{l=1}^{q} \sum_{j=2}^{\lambda_l} \chi_{l,j}^{\kappa,i} \theta^{\sigma_j^l} - \sigma_i^\kappa \left\| \bar{e}_j^l \right\|.
\end{aligned} \tag{43}$$

This yields to

$$\begin{aligned}
\dot{V}_\kappa\left(\bar{e}^\kappa\right) &\leq -\theta^{\delta_\kappa} V_\kappa\left(\bar{e}^\kappa\right) + 2L_{\tilde{\varphi}^\kappa} \mu_s \sqrt{V_\kappa\left(\bar{e}^\kappa\right)} \\
&\quad \times \sum_{i=1}^{\lambda_\kappa} \sum_{l=1}^{q} \sum_{j=2}^{\lambda_l} \chi_{l,j}^{\kappa,i} \theta^{\sigma_j^l - \sigma_i^\kappa} \sqrt{V_l(\bar{e}_l)} \\
&= -\theta^{\delta_\kappa} V_\kappa\left(\bar{e}^\kappa\right) + 2L_{\tilde{\varphi}^\kappa} \mu_s \sqrt{\theta^{\delta_\kappa} V_\kappa\left(\bar{e}^\kappa\right)} \\
&\quad \times \sum_{i=1}^{\lambda_\kappa} \sum_{l=1}^{q} \sum_{j=2}^{\lambda_l} \chi_{l,j}^{\kappa,i} \theta^{\sigma_j^l - \sigma_i^\kappa - \frac{\delta_l}{2} - \frac{\delta_\kappa}{2}} \sqrt{\theta^{\delta_l} V_l(\bar{e}_l)},
\end{aligned} \tag{44}$$

where $\mu_s = \sqrt{\overline{\lambda}_S / \underline{\lambda}_S}$ with

$$\overline{\lambda}_S = \max_{\kappa=1,\ldots,q} \overline{\lambda}_M(S_\kappa) \text{and} \underline{\lambda}_S = \min_{\kappa=1,\ldots,q} \underline{\lambda}_m(S_\kappa). \tag{45}$$

Otherwise, according to Lemma 2.1, one has:

$$\sigma_j^l - \sigma_i^\kappa - \frac{\delta_l}{2} - \frac{\delta_\kappa}{2} \leq -\frac{\eta}{2^q} \text{if} \chi_{l,j}^{\kappa,i} = 1. \tag{46}$$

And using (46) together with (44) yields

$$\begin{aligned}
\dot{V}_\kappa\left(\bar{e}^\kappa\right) &\leq -\theta^{\delta_\kappa} V_\kappa\left(\bar{e}^\kappa\right) + 2L_{\tilde{\varphi}^\kappa} \mu_s \theta^{-\eta/2^q} \sqrt{\theta^{\delta_\kappa} V_\kappa\left(\bar{e}^\kappa\right)} \\
&\quad \times \sum_{i=1}^{\lambda_\kappa} \sum_{l=1}^{q} \sum_{j=2}^{\lambda_l} \sqrt{\theta^{\delta_l} V_l(\bar{e}_l)}.
\end{aligned} \tag{47}$$

Furthermore, let

$$V_\kappa^*\left(\bar{e}^\kappa\right)=\theta^{\delta_\kappa}V_\kappa\left(\bar{e}^\kappa\right)\ \text{ and }\ V^*\left(\bar{e}\right)=\sum_{\kappa=1}^{q}V_\kappa^*\left(\bar{e}^\kappa\right), \tag{48}$$

and using (9), one has: $V^*(\bar{e})\geq\theta^{\delta q}V(\bar{e})=\theta V(\bar{e})$. This allows to rewrite inequality (47) as follows

$$\begin{aligned}
\dot{V}_\kappa\left(\bar{e}^\kappa\right)&\leq -V_\kappa^*\left(\bar{e}\right)+2L_{\tilde{\varphi}^\kappa}\mu_s\theta^{-\eta/2^q}\sqrt{V_\kappa^*\left(\bar{e}^\kappa\right)}\\
&\quad\times\sum_{i=1}^{\lambda_\kappa}\sum_{l=1}^{q}\sum_{j=2}^{\lambda_l}\sqrt{V_l^*\left(\bar{e}^\kappa\right)}\\
&=-V_\kappa^*\left(\bar{e}^\kappa\right)+2L_{\tilde{\varphi}^\kappa}\mu_s\lambda_\kappa\theta^{-\eta/2^q}\sqrt{V_\kappa^*\left(\bar{e}\right)\left(\bar{e}^\kappa\right)}\\
&\quad\times\sum_{l=1}^{q}\sum_{j=2}^{\lambda_l}\sqrt{V_l^*\left(\bar{e}_l\right)}\\
&\leq -V_\kappa^*\left(\bar{e}^\kappa\right)+2L_{\tilde{\varphi}^\kappa}\mu_s\lambda_\kappa\theta^{-\eta/2^q}\sqrt{V_\kappa^*\left(\bar{e}^\kappa\right)\left(\bar{e}^\kappa\right)}\\
&\quad\times\sum_{l=1}^{q}\sum_{j=2}^{\lambda_l}\sqrt{V^*\left(\bar{e}^\kappa\right)}\\
&\leq -V_\kappa^*\left(\bar{e}^\kappa\right)\\
&\quad+2nL_{\tilde{\varphi}^\kappa}\mu_s\lambda_\kappa\theta^{-\eta/2^q}\sqrt{V_\kappa^*\left(\bar{e}^\kappa\right)}\sqrt{V^*\left(\bar{e}\right)}\\
&\leq -V_\kappa^*\left(\bar{e}^\kappa\right)+2nL_{\tilde{\varphi}^\kappa}\mu_s\lambda_\kappa\theta^{-\eta/2^q}V^*\left(\bar{e}\right).
\end{aligned}$$

This leads to

$$\begin{aligned}
\dot{V}\left(\bar{e}\right)&\leq -V^*\left(\bar{e}\right)+2n^2L_{\tilde{\varphi}}\mu_s\theta^{-\frac{\eta}{2^q}}V^*\left(\bar{e}\right)\\
&=-\left(1-2n^2L_{\tilde{\varphi}}\mu_s\theta^{-\frac{\eta}{2^q}}\right)V^*\left(\bar{e}\right),
\end{aligned}\tag{49}$$

where $L_{\tilde{\varphi}}=\max\{L_{\tilde{\varphi}^\kappa}\ \textit{for}\ 1\leq\kappa\leq q\}$ And according to (30) and (49), one gets

$$\dot{V}\left(\bar{e}\right)\leq-\theta\left(1-\sqrt{\frac{\alpha(\theta)}{\theta^{\frac{\eta}{2^{q-1}}}}}\sqrt{\frac{n^4e\overline{\lambda_M\left(S\right)}}{\delta_o}}L_{\tilde{\varphi}}\right)V\left(\bar{e}\right). \tag{50}$$

From (23), it is easy to check that for values of θ sufficiently large, $V(\bar{e})$ exponentially converges to zero and so does $\bar{e}$. This ends the proof of Theorem 3.1. ■

4. The continuous-discrete time observer

In this section, one aims at providing a continuous-discrete time observer for the considered class of systems in the spirit of the design approach proposed in Farza et al. (2014). This consists in performing an accurate continuous-time estimation of the system state when the output measurements are available only at sampling time instants $\{t_k\}_{k\in\mathbb{N}}$ by appropriately redesigning continuous-time observer proposed in Section 3 as follows:

$$\begin{aligned}
\dot{\hat{x}}^\kappa\left(t\right)&=A_\kappa\left(u(t)\right)\hat{x}^\kappa(t)+\varphi^\kappa\left(u(t),\underline{\hat{x}}(t)\right)\\
&\quad-\theta^{\delta^\kappa}\Delta_\kappa^{-1}\left(\theta\right)S_\kappa^{-1}\left(t\right)C_\kappa^T\eta_\kappa\left(t\right)\\
\dot{S}_\kappa\left(t\right)&=\theta^{\delta_\kappa}\Big(-S_\kappa\left(t\right)-A_\kappa^T\left(u(t)\right)S_\kappa\left(t\right)\\
&\quad-S_\kappa\left(t\right)A_\kappa\left(u(t)\right)+C_\kappa^TC_\kappa\Big)\\
\dot{\eta}_\kappa\left(t\right)&=-\theta^{\delta_\kappa}C_\kappa S_\kappa^{-1}\left(t\right)C_\kappa^T\eta_\kappa\left(t\right)\quad \textit{for}\ t\in[t_k,t_{k+1}[\\
\eta_\kappa\left(t_k\right)&=C_\kappa\hat{x}^\kappa\left(t_k\right)-y_\kappa\left(t_k\right),
\end{aligned}\tag{51}$$

where $\hat{x}^\kappa(t)$ denotes the estimate of the block state $x^\kappa(t)\in\mathbb{R}^{n_\kappa}$ for $\kappa=1,\ldots,q$ and $\Delta_\kappa(\theta)$ is the block-diagonal matrix defined in (6) with $\theta>1$.

It is worth noticing that the function η_κ is continuous over the time horizon $[t_k,t_{k+1}[$ and is updated at each sampling instant t_k using only the sampled output measurement $y_\kappa(t_\kappa)$. The dynamical system (51) performs hence a continuous-time estimation of the system state from the sampled output measurements. And the involved estimation is accurate as pointed out by the following result.

Theorem 4.1: *Consider system* (1) *subject to assumptions* **A1** *and* **A2** *with an input sequence* $\{u(t)\}$ *satisfying assumption* **A3**. *Then, there exists* $\theta_o>1$ *such that for every* $\theta\geq\theta_o$, *there exists* $\chi_\theta>0$ *such that if the upper bound of the sampling partition parameter* $\tau_{\max}$ *is chosen such that*

$$\tau_{\max}<\chi_\theta, \tag{52}$$

then the state of the continuous time observer with sampled measurements (51)*converges exponentially toward the state of the nonlinear system* (1).

Proof of Theorem 2: Set $\bar{e}^\kappa=\Lambda_\kappa(\theta)\tilde{e}^\kappa$ where $\tilde{e}^\kappa=\hat{x}^\kappa-x^\kappa$. Using (1) and (51), one gets

$$\begin{aligned}
\dot{\tilde{e}}^\kappa\left(t\right)&=\theta^{\delta_\kappa}\left(A_\kappa(u)-S_\kappa^{-1}C_\kappa^TC_\kappa\right)\tilde{e}^\kappa\\
&\quad+\theta^{\delta_\kappa}S_\kappa^{-1}C_\kappa^Tz_\kappa(t)+\Lambda_\kappa\left(\theta\right)\tilde{\varphi}^\kappa\left(u,\underline{\hat{x}},x\right),
\end{aligned}\tag{53}$$

with$z_\kappa(t)=C_\kappa\bar{e}^\kappa(t)-\eta_\kappa(t)$ and $\tilde{\varphi}^\kappa(u(t),\underline{\hat{x}}(t),x(t))=\varphi^\kappa(u(t),\hat{x}(t))-\varphi(u(t),x(t))$.

The exponential convergence of the observation error can be proven using the following Lyapunov function candidate

$$\begin{aligned}
V(\bar{e})&=\sum_{k=1}^{q}V_\kappa\left(\bar{e}^\kappa\right)\quad\text{with}\\
V_\kappa\left(\bar{e}^\kappa(t)\right)&=\left(\bar{e}^\kappa(t)\right)^TS_\kappa(t)\bar{e}^\kappa(t).
\end{aligned}\tag{54}$$

Differentiating the Lyapunov function candidate, taking into account the normalised observation error equation (53) yields

$$\begin{aligned}\dot{V}_\kappa\left(\bar{e}^\kappa\right) &= -\theta^{\delta_\kappa} V_\kappa\left(\bar{e}^\kappa\right) - \theta^{\delta_\kappa}\left(\bar{e}^\kappa\right)^T C_\kappa^T C_\kappa \bar{e}^\kappa \\ &\quad + 2\theta^{\delta_\kappa}\left(\bar{e}^\kappa\right)^T C_\kappa^T z_\kappa \\ &\quad + 2\left(\bar{e}^\kappa\right)^T S_\kappa \Lambda_\kappa(\theta)\,\tilde{\varphi}^\kappa\left(u,\underline{\hat{x}},x\right). \end{aligned} \tag{55}$$

And using the ODE proving $\eta_\kappa(t)$ in the observer (51), one can show that

$$\dot{z}_\kappa\left(\bar{e}^\kappa\right) = C_\kappa\left(\theta^{\delta_\kappa} A_\kappa(u)\,\bar{e}^\kappa(t) + \Lambda_\kappa(\theta)\,\tilde{\varphi}^\kappa\left(u,\underline{\hat{x}},x\right)\right). \tag{56}$$

Otherwise, integrating the members of (56) from t_κ to t, using the fact that $z(t_\kappa)=0$, one obtains

$$\begin{aligned} z_\kappa(t) = \int_{t_\kappa}^{t} & C_\kappa\left(\theta^{\delta_\kappa} A_\kappa(u)\,\bar{e}^\kappa(s)\right. \\ & \left. + \Lambda_\kappa(\theta)\,\tilde{\varphi}^\kappa\left(u,\underline{\hat{x}},x\right)\right)\mathrm{d}s. \end{aligned} \tag{57}$$

This allows to obtain an over-evaluation of $\|z_\kappa(t)\|$ according to the following manipulations

$$\begin{aligned}\|z_\kappa\| &\le \left(\theta^{\delta_\kappa}\int_{t_\kappa}^{t}\|C_\kappa A_\kappa(u)\|\left\|\bar{e}^\kappa\right\|\mathrm{d}s\right. \\ &\quad \left. + \int_{t_\kappa}^{t}\sum_{i=1}^{\lambda_\kappa}\frac{1}{\theta^{\sigma_i^\kappa}}\left\|\tilde{\varphi}_i^\kappa\left(u,\underline{\hat{x}},x\right)\right\|\mathrm{d}s\right) \\ &\le \left(\theta^{\delta_\kappa}\tilde{a}_\kappa\int_{t_\kappa}^{t}\left\|\bar{e}^\kappa\right\|\mathrm{d}s\right. \\ &\quad \left. + L_{\tilde{\varphi}^\kappa}\int_{t_\kappa}^{t}\sum_{i=1}^{\lambda_\kappa}\sum_{l=1}^{q}\sum_{j=2}^{\lambda_l}\chi_{l,j}^{k,i}\theta^{-\sigma_i^\kappa}\left\|\bar{e}_j^l\right\|\mathrm{d}s\right) \\ &\le \left(\theta^{\delta_\kappa}\tilde{a}_\kappa\int_{t_\kappa}^{t}\left\|\bar{e}^\kappa\right\|\mathrm{d}s\right. \\ &\quad \left. + L_{\tilde{\varphi}^\kappa}\int_{t_\kappa}^{t}\sum_{i=1}^{\lambda_\kappa}\sum_{l=1}^{q}\sum_{j=2}^{\lambda_l}\chi_{l,j}^{\kappa,i}\theta^{\sigma_j^l-\sigma_i^\kappa}\left\|\bar{e}_j^l\right\|\mathrm{d}s\right) \\ &\le \frac{1}{\sqrt{\underline{\lambda}_S}}\left(\theta^{\delta_\kappa}\tilde{a}_\kappa\int_{t_\kappa}^{t}\sqrt{V_\kappa}\,\mathrm{d}s\right. \\ &\quad \left. + L_{\tilde{\varphi}^\kappa}\int_{t_\kappa}^{t}\sum_{i=1}^{\lambda_\kappa}\sum_{l=1}^{q}\sum_{j=2}^{\lambda_l}\chi_{l,j}^{\kappa,i}\theta^{\sigma_j^l-\sigma_i^\kappa}\sqrt{V_l}\,\mathrm{d}s\right), \end{aligned} \tag{58}$$

where $\tilde{a}^\kappa$ and $\underline{\lambda_S}$ are respectively defined by (5) and (45).

Moreover, one has

$$\begin{aligned}&\|2\theta^{\delta_\kappa}\bar{e}^\kappa C_\kappa^T z_\kappa\| \\ &\le 2\theta^{\delta_\kappa}\mu_S\sqrt{V_\kappa}\left(\theta^{\delta_\kappa}\tilde{a}_\kappa\int_{t_\kappa^t}\sqrt{V_\kappa}\,\mathrm{d}s\right. \\ &\quad \left. + L_{\tilde{\varphi}^\kappa}\int_{t_\kappa^t}\sum_{i=1}^{\lambda_\kappa}\sum_{l=1}^{q}\sum_{j=2}^{\lambda_l}\chi_{l,j^{\kappa,i}}\theta^{\sigma_j^l-\sigma_i^\kappa}\sqrt{V_l}\,\mathrm{d}s\right) \\ &\le 2\theta^{\delta_\kappa}\mu_s\sqrt{V_\kappa}\left(\theta^{\delta_\kappa}\tilde{a}_\kappa\int_{t_\kappa}^{t}\sqrt{V_\kappa}\,\mathrm{d}s\right. \\ &\quad \left. + L_{\tilde{\varphi}^\kappa}\int_{t_\kappa}^{t}\sum_{i=1}^{\lambda_\kappa}\sum_{l=1}^{q}\sum_{j=2}^{\lambda_l}\chi_{l,j}^{k,i}\theta^{\sigma_j^l-\sigma_i^\kappa}\sqrt{V_l}\,\mathrm{d}s\right), \end{aligned} \tag{59}$$

where $\mu_S = \sqrt{\overline{\lambda_S}/\underline{\lambda_S}}$ where $\overline{\lambda_S}$ and $\underline{\lambda_S}$ are defined by (45). And substituting (59) into (55) yields

$$\begin{aligned}\dot{V}_\kappa &\le -\theta^{\delta_\kappa}V_\kappa + 2\sqrt{\overline{\lambda_S}}\sqrt{V_\kappa}\left(\sum_{i=1}^{\lambda_\kappa}\theta^{-\sigma_i^\kappa}\left\|\tilde{\varphi}_i^\kappa\left(u,\hat{x},x\right)\right\|\right) \\ &\quad + 2\theta^{\delta_\kappa}\mu_s\sqrt{V_\kappa}\left(\theta^{\delta_\kappa}\tilde{a}_\kappa\int_{t_\kappa}^{t}\sqrt{V_\kappa}\,\mathrm{d}s\right. \\ &\quad \left. + L_{\tilde{\varphi}^\kappa}\int_{t_\kappa}^{t}\sum_{i=1}^{\lambda_\kappa}\sum_{l=1}^{q}\sum_{j=2}^{\lambda_l}\chi_{l,j}^{\kappa,i}\theta^{\sigma_j^l-\sigma_i^\kappa}\sqrt{V_l}\,\mathrm{d}s\right). \end{aligned} \tag{60}$$

Otherwise, according to assumption **A1** and the property of $\chi_{l,j}^{k,i}$ given by Lemma 2.1, one can easily obtain

$$\begin{aligned}\dot{V}_\kappa &\le -\theta^{\delta_\kappa}V_\kappa \\ &\quad + 2L_{\tilde{\varphi}^\kappa}\sqrt{\overline{\lambda_S}}\sqrt{V_\kappa}\sum_{i=1}^{\lambda_\kappa}\sum_{l=1}^{q}\sum_{j=2}^{\lambda_l}\chi_{l,j}^{\kappa,i}\theta^{\sigma_j^l-\sigma_i^\kappa}\left\|\bar{e}_j^l\right\| \\ &\quad + 2\theta^{\delta_\kappa}\mu_s\sqrt{V_\kappa}\left(\theta^{\delta_\kappa}\tilde{a}_\kappa\int_{t_\kappa}^{t}\sqrt{V_\kappa}\,\mathrm{d}s\right. \\ &\quad \left. + L_{\tilde{\varphi}^\kappa}\int_{t_\kappa}^{t}\sum_{i=1}^{\lambda_\kappa}\sum_{l=1}^{q}\sum_{j=2}^{\lambda_l}\chi_{l,j}^{\kappa,i}\theta^{\sigma_j^l-\sigma_i^\kappa}\sqrt{V_l}\,\mathrm{d}s\right), \end{aligned} \tag{61}$$

where σ_j^l is defined as in (11). And pursuing these developments, one gets

$$\begin{aligned}\dot{V}_\kappa &\le -\theta^{\delta_\kappa}V_\kappa \\ &\quad + 2L_{\tilde{\varphi}^\kappa}\mu_s\sqrt{V_\kappa}\sum_{i=1}^{\lambda_\kappa}\sum_{l=1}^{q}\sum_{j=2}^{\lambda_l}\chi_{l,j}^{\kappa,i}\theta^{\sigma_j^l-\sigma_i^\kappa}\sqrt{V_l} \end{aligned}$$

$$
\begin{aligned}
&+ 2\theta^{\delta_\kappa}\mu_s\sqrt{V_\kappa}\left(\theta^{\delta_\kappa}\tilde{a}_\kappa\int_{t_\kappa}^{t}\sqrt{V_\kappa}\,\mathrm{d}s\right.\\
&\left.+ L_{\tilde{\varphi}^\kappa}\int_{t_\kappa}^{t}\sum_{i=1}^{\lambda_\kappa}\sum_{l=1}^{q}\sum_{j=2}^{\lambda_l}\chi_{l,j}^{\kappa,i}\theta^{\sigma_j^l-\sigma_i^\kappa}\sqrt{V_l}\,\mathrm{d}s\right)\\
&\leq -\theta^{\delta_\kappa}V_\kappa + 2L_{\tilde{\varphi}^\kappa}\mu_s\sqrt{\theta^{\delta_\kappa}V_\kappa}\\
&\quad\times\sum_{i=1}^{\lambda_\kappa}\sum_{l=1}^{q}\sum_{j=2}^{\lambda_l}\chi_{l,j}^{\kappa,i}\theta^{\sigma_j^l-\sigma_i^\kappa-\frac{1}{2}\delta_l-\frac{1}{2}\delta_\kappa}\sqrt{\theta^{\delta_l}V_l}\,\mathrm{d}s\\
&\quad+ 2\theta^{\delta_\kappa}\mu_s\sqrt{\theta^{\delta_\kappa}V_\kappa}\left(\tilde{a}_\kappa\int_{t_\kappa}^{t}\sqrt{\theta^{\delta_\kappa}V_\kappa}\,\mathrm{d}s + L_{\tilde{\varphi}^\kappa}\int_{t_\kappa}^{t}\right.\\
&\quad\left.\times\sum_{i=1}^{\lambda_\kappa}\sum_{l=1}^{q}\sum_{j=2}^{\lambda_l}\chi_{l,j}^{\kappa,i}\theta^{\sigma_j^l-\sigma_i^\kappa-\frac{1}{2}\delta_l-\frac{1}{2}\delta_\kappa}\sqrt{\theta^{\delta_l}V_l}\,\mathrm{d}s\right).
\end{aligned}
\tag{62}
$$

Applying Lemma 2.1 and using Equation (46), one obtains

$$
\begin{aligned}
\dot{V}_\kappa &\leq -\theta^{\delta_\kappa}V_\kappa + 2L_{\tilde{\varphi}^\kappa}\mu_s\theta^{-\frac{\eta}{2q}}\sqrt{\theta^{\delta_\kappa}V_\kappa}\\
&\quad\times\sum_{i=1}^{\lambda_\kappa}\sum_{l=1}^{q}\sum_{j=2}^{\lambda_l}\sqrt{\theta^{\delta_l}V_l}\\
&\quad+ 2\theta^{\delta_\kappa}\mu_s\left(\tilde{a}_\kappa\int_{t_\kappa}^{t}\sqrt{\theta^{\delta_\kappa}V_\kappa}\,\mathrm{d}s + \theta^{-\frac{\eta}{2q}}L_{\tilde{\varphi}^\kappa}\right.\\
&\quad\left.\times\int_{t_\kappa}^{t}\sum_{i=1}^{\lambda_\kappa}\sum_{l=1}^{q}\sum_{j=2}^{\lambda_l}\sqrt{\theta^{\delta_l}V_l}\,\mathrm{d}s\right)\sqrt{\theta^{\delta_\kappa}V_\kappa}.
\end{aligned}
\tag{63}
$$

Now, let us consider the functions V_κ^* and V^* defined by (48), one has:

$$
\begin{aligned}
\dot{V}_\kappa &\leq -V_\kappa^* + 2L_{\tilde{\varphi}^\kappa}\mu_s\theta^{-\frac{\eta}{2q}}\sqrt{V_\kappa^*}\sum_{i=1}^{\lambda_\kappa}\sum_{l=1}^{q}\sum_{j=2}^{\lambda_l}\sqrt{V_l^*}\\
&\quad+ 2\theta^{\delta_\kappa}\mu_s\left(\tilde{a}_\kappa\int_{t_\kappa}^{t}\sqrt{V_\kappa^*}\,\mathrm{d}s\right.\\
&\quad\left.+\theta^{-\frac{\eta}{2q}}L_{\tilde{\varphi}^\kappa}\int_{t_\kappa}^{t}\sum_{i=1}^{\lambda_\kappa}\sum_{l=1}^{q}\sum_{j=2}^{\lambda_l}\sqrt{V_l^*}\,\mathrm{d}s\right)\sqrt{V_\kappa^*}\\
&= -V_\kappa^* + 2\lambda_\kappa L_{\tilde{\varphi}^\kappa}\mu_s\theta^{-\frac{\eta}{2q}}\sqrt{V_\kappa^*}\sum_{i=1}^{q}\sum_{l=1}^{\lambda_\kappa}\sqrt{V_l^*}\\
&\quad+ 2\theta^{\delta_\kappa}\mu_s\left(\tilde{a}_\kappa\int_{t_\kappa}^{t}\sqrt{V_\kappa^*}\,\mathrm{d}s\right.\\
&\quad\left.+\lambda_\kappa\theta^{-\frac{\eta}{2q}}L_{\tilde{\varphi}^\kappa}\int_{t_\kappa}^{t}\sum_{i=1}^{q}\sum_{l=1}^{\lambda_\kappa}\sqrt{V_l^*}\,\mathrm{d}s\right)\sqrt{V_\kappa^*}\\
&\leq -V_\kappa^* + 2\lambda_\kappa L_{\tilde{\varphi}^\kappa}\mu_s\theta^{-\frac{\eta}{2q}}\sqrt{V_\kappa^*(\bar{e}^\kappa)}\sum_{i=1}^{q}\sum_{l=1}^{\lambda_\kappa}\sqrt{V^*}\\
&\quad+ 2\theta^{\delta_\kappa}\mu_s\left(\tilde{a}_\kappa\int_{t_\kappa}^{t}\sqrt{V_\kappa^*}\,\mathrm{d}s\right.\\
&\quad\left.+\lambda_\kappa\theta^{-\frac{\eta}{2q}}L_{\tilde{\varphi}^\kappa}\int_{t_\kappa}^{t}\sum_{i=1}^{q}\sum_{l=1}^{\lambda_\kappa}\sqrt{V_l^*}\,\mathrm{d}s\right)\sqrt{V_\kappa^*}\\
&\leq -V_\kappa^* + 2n\lambda_\kappa L_{\tilde{\varphi}^\kappa}\mu_s\theta^{-\frac{\eta}{2q}}\sqrt{V_\kappa^*}\sqrt{V^*}\\
&\quad+ 2\theta^{\delta_\kappa}\mu_s\left(\tilde{a}_\kappa\int_{t_\kappa}^{t}\sqrt{V_\kappa^*}\,\mathrm{d}s\right.\\
&\quad\left.+ n\lambda_\kappa\theta^{-\frac{\eta}{2q}}L_{\tilde{\varphi}^\kappa}\int_{t_\kappa}^{t}\sqrt{V^*}\,\mathrm{d}s\right)\sqrt{V_\kappa^*}\\
&\leq -V_\kappa^* + 2n\lambda_\kappa L_{\tilde{\varphi}^\kappa}\mu_s\theta^{-\frac{\eta}{2q}}V_\kappa^*(\bar{e}^\kappa)\\
&\quad+ 2\theta^{\delta_\kappa}\mu_s\left(\tilde{a}_\kappa\int_{t_\kappa}^{t}\sqrt{V_\kappa}\,\mathrm{d}s\right.\\
&\quad\left.+ n\lambda_\kappa\theta^{-\frac{\eta}{2q}}L_{\tilde{\varphi}^\kappa}\int_{t_\kappa}^{t}\sqrt{V^*}\,\mathrm{d}s\right)\sqrt{V_\kappa^*}.
\end{aligned}
\tag{64}
$$

Taking into account (46) and (48), one obtains

$$
\begin{aligned}
\dot{V}_\kappa &\leq -V_\kappa^* + 2n\lambda_\kappa L_{\tilde{\varphi}^\kappa}\mu_s\theta^{-\frac{\eta}{2q}}V_\kappa^* + 2\theta^{\delta_1}\mu_s\\
&\quad\times\left(\left(\tilde{a}_\kappa\lambda_\kappa + n\lambda_\kappa\theta^{-\frac{\eta}{2q}}L_{\tilde{\varphi}^\kappa}\right)\int_{t_\kappa}^{t}\sqrt{V_\kappa^*}\,\mathrm{d}s\right)\sqrt{V_\kappa^*}.
\end{aligned}
\tag{65}
$$

And henceforth

$$
\begin{aligned}
\dot{V} &= -\left(1 - 2n^2L_{\tilde{\varphi}}\mu_s\theta^{-\frac{\eta}{2q}}\right)V^*\\
&\quad+ 2\theta^{\delta_{[l]}}\mu_s\left(\left(\tilde{a} + n^2\theta^{-\frac{\eta}{2q}}L_{\tilde{\varphi}}\right)\int_{t_\kappa}^{t}\sqrt{V^*}\,\mathrm{d}s\right)\sqrt{V^*},
\end{aligned}
$$

where $\tilde{a} = \max_{1\leq k\leq q}\tilde{a}_\kappa$.

The above equation can be written as follows

$$
\begin{aligned}
\frac{\mathrm{d}\sqrt{V}}{\mathrm{d}t} &= -\left(1 - 2n^2L_{\tilde{\varphi}}\mu_s\theta^{-\eta/2q}\right)\sqrt{V^*}\\
&\quad+ 2\theta^{\delta_1}\mu_s\left(\tilde{a} + n^2\theta^{-\frac{\eta}{2q}}L_{\tilde{\varphi}}\right)\int_{t_\kappa}^{t}\sqrt{V^*}\,\mathrm{d}s,
\end{aligned}
\tag{66}
$$

where the argument of the functions V and V^* have been omitted. And using (30) and $V^*(\bar{e})$, it follows that:

$$
\frac{\mathrm{d}}{\mathrm{d}t}\left(\sqrt{V}\right) = -\sqrt{\theta}\left(1 - 2\sqrt{\frac{\alpha(\theta)}{\theta^{\frac{\eta}{2^{q-1}}}}}\sqrt{\frac{n^4e\lambda_M(S)}{\delta_o}L_{\tilde{\varphi}}}\right)\sqrt{V}
$$

$$+ 2\theta^{\delta_1}\sqrt{\frac{\theta\alpha(\theta)e\lambda_M}{\delta_o}}$$
$$\times\left(\tilde{a} + n^2\theta^{-\frac{\eta}{2q}}L_{\tilde{\varphi}}\right)\int_{t_\kappa}^{t}\sqrt{V}\,\mathrm{d}s. \tag{67}$$

Finally, using Lemma 2.2 with

$$a_\theta = \left(1 - 2\sqrt{\frac{\alpha(\theta)}{\theta^{\frac{\eta}{2q-1}}}}\sqrt{\frac{n^4 e\lambda_M(S)}{\delta_o}}L_{\tilde{\varphi}}\right) \quad \text{and}$$
$$b_\theta = 2\theta^{\delta_1}\sqrt{\frac{\theta\alpha(\theta)e\lambda_M}{\delta_o}}\left(\tilde{a} + n^2\theta^{-\frac{\eta}{2q}}L_{\tilde{\varphi}}\right),$$

and defining $\chi_\theta = a_\theta/b_\theta$, on gets the result. ■

5. Application to an unmanned aerial vehicle

In the following, one shall show that the proposed continuous-discrete time observer can be used to provide an accurate estimation of the quadrotor state variables, namely the position and Euler angles together with their respective speeds, using only sampled measurements of the position and the yaw angle. Such an estimation is carried out using a realistic simulation framework involving a quadrotor dynamical model describing its barycentre movements and angular motions, namely the three translation and three rotation motions provided by the six degree of freedom of the quadrotor. This model is obtained using the inertial coordinate frame and a mobile reference frame united with the quadrotor barycentre as shown in Figure 1. The rotation from the mobile reference frame to the inertial position frame is described by the following rotational matrix

$$R = \begin{bmatrix} c_\psi c_\theta & -s_\psi c_\theta & s_\theta \\ c_\psi s_\theta s_\phi + s_\psi c_\phi & -s_\psi s_\theta s_\phi + c_\psi c_\phi & -c_\theta s_\phi \\ -c_\psi s_\theta c_\phi + s_\psi s_\phi & s_\psi s_\theta c_\phi + c_\psi s_\phi & c_\theta c_\phi \end{bmatrix}$$

with $s_\eta = \sin(\eta)$ and $c_\eta = \cos(\eta)$ for $\eta = \theta, \phi, \psi$, where θ, ϕ and ψ denote the Euler angles, i.e. the roll, pitch and yaw, respectively.

The configuration variables are then given by the position of the quadrotor centre of mas in the inertial reference frame and the space quadrotor orientation and are hence given by $v = [\varpi\ \theta] \in \mathbb{R}^6$ with $\varpi = [x\ y\ z] \in \mathbb{R}^3$ and $\vartheta = [\phi\ \theta\ \psi] \in \mathbb{R}^3$.

Otherwise, the control inputs of the quadrotor are the force resulting from the forces provided by the each rotor and the torques applied to each axis, i.e. $u = [f\ \tau]^{\mathrm{T}} \in \mathbb{R}^4$ with $\tau = [\tau_\phi\ \tau_\theta\ \tau_\psi]^{\mathrm{T}} \in \mathbb{R}^3$. The modelling process of the quadrotor is comprehensively presented in Guisser and Medromi (2009) where it has been shown that

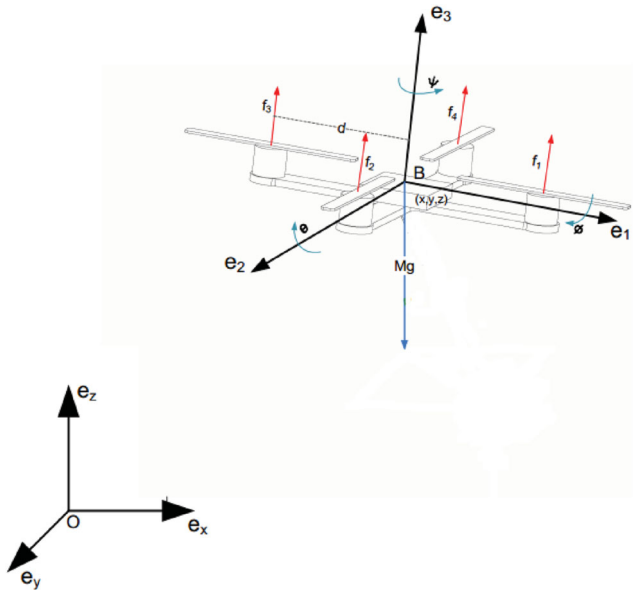

Figure 1. 3D Quadrotor UAV.

the underlying translational and rotational motions are described by the dynamical model

$$\ddot{\varpi} = \begin{bmatrix} 0 \\ 0 \\ -g \end{bmatrix} + \begin{bmatrix} \sin(\theta) \\ -\cos(\theta)\sin(\phi) \\ \cos(\theta)\cos(\phi) \end{bmatrix}\frac{f}{m}$$
$$\ddot{\vartheta} = \begin{bmatrix} a_1\dot{\theta}\dot{\psi} + b_1\tau_\phi \\ a_2\dot{\phi}\dot{\psi} + b_2\tau_\theta \\ a_3\dot{\theta}\dot{\phi} + b_3\tau_\psi \end{bmatrix}, \tag{68}$$

where m is the mass of the quadrotor system, g is the gravity acceleration and the parameters a_1, a_2, a_3, b_1, b_2 and b_3 are defined as follows

$$a_1 = \frac{I_y - I_z}{I_x}, \quad a_2 = \frac{I_z - I_x}{I_y}, \quad a_3 = \frac{I_x - I_y}{I_z},$$
$$b_1 = \frac{1}{I_x}, \quad b_2 = \frac{1}{I_y}, \quad b_3 = \frac{1}{I_z},$$

where I_x, I_y and I_z are the mass moments of inertia of the quadrotor in the inertial coordinate frame.

Otherwise, the choice of the measured output is of a fundamental interest from the observer design point of view, namely ensure that the observer design is feasible while avoiding the use of expensive motion capture systems, such as VICON or OptiTrack systems. As the position and the raw angle of the quadrotor can be respectively measured by a Global Positioning System (GPS) and a digital compass, as was considered in Shao et al. (2018), they can be used to compose the system output $\mu = [\mu_1\ \mu_2\ \mu_3\ \mu_4]^{\mathrm{T}} = [x\ y\ z\ \psi]^{\mathrm{T}} \in \mathbb{R}^4$.

In the following, one shall show that the quadrotor model (68) can be rewritten under the form (20)

up to the following change of coordinates $\Phi : \xi \in \mathcal{X} \subset \mathbb{R}^{12} \to \zeta = \Phi(\xi) \in \mathcal{Z} \subset \mathbb{R}^{12}$ where $\mathcal{X}$ and $\mathcal{Z}$ are respectively compact sets of $\mathbb{R}^{12}$ and $\xi \in \mathcal{X} \subset \mathbb{R}^{12}$ $\zeta \in \mathcal{Z} \subset \mathbb{R}^{12}$ respectively denote the original and new coordinates defined as follows: $\xi = [\xi^1 \ \xi^2 \ \xi^3 \ \xi^4]^{\mathrm{T}} = [\varpi \ \dot{\varpi} \ \vartheta \ \dot{\vartheta}]^{\mathrm{T}} \in \mathbb{R}^{12}$, and $\zeta = [\zeta^1, \zeta^2, \zeta^3, \zeta^4]^{\mathrm{T}} \in \mathbb{R}^{12}$ with $\zeta^j = [\zeta_1^j, \zeta_2^j, \zeta_3^j, \zeta_4^j]^{\mathrm{T}}$ for $j = 1,2$ and $\zeta^i = [\zeta_1^i \ \zeta_2^i]$ for $i = 3, 4$, with

$$\begin{aligned}
\zeta^1 &= \left[x\ \dot{x}\ \sin(\theta)\ \dot{\theta}\sin(\theta)\right]^T, \\
\zeta^2 &= \begin{bmatrix} y \\ \dot{y} \\ -\cos(\theta)\sin(\phi) \\ \dot{\theta}\sin(\theta)\sin(\phi) - \dot{\phi}\cos(\theta)\cos(\phi) \end{bmatrix}, \\
\zeta^3 &= \left[z\ \dot{z}\right]^T \quad \text{and} \quad \zeta^4 = \left[\psi\ \dot{\psi}\right]^T.
\end{aligned} \tag{69}$$

Taking into account the above state decomposition of the vectors ξ and ζ together with the considered measurement output decomposition μ, one can easily show that the quadrotor model can be rewritten under the form of the system (20) with the structure values $q = 4, p_1 = p_2 = p_3 = p_4 = 1, \lambda_1 = \lambda_2 = 4$ and $\lambda_3 = \lambda_4 = 2$, namely

$$\begin{aligned}
\dot{\zeta}^\kappa(t) &= A_\kappa\,(u(t))^\kappa\,(t) + \varphi^\kappa\,(u(t), \zeta(t)) \\
\mu_k(t) &= C_\kappa \zeta^\kappa\,(t)
\end{aligned} \tag{70}$$

with

$$A_1(u) = \begin{bmatrix} 0 & 1 & 0 & 0 \\ 0 & 0 & \dfrac{f}{m} & 0 \\ 0 & 0 & 0 & 1 \\ 0 & 0 & 0 & 0 \end{bmatrix},$$

$$\varphi^1(\zeta, u) = \begin{bmatrix} 0 \\ 0 \\ 0 \\ \varphi_4^1(\zeta, u) \end{bmatrix} \quad \text{and} \quad C_1 = \begin{bmatrix} 1 & 0 & 0 & 0 \end{bmatrix},$$

$$A_2(u) = \begin{bmatrix} 0 & 1 & 0 & 0 \\ 0 & 0 & \dfrac{f}{m} & 0 \\ 0 & 0 & 0 & 1 \\ 0 & 0 & 0 & 0 \end{bmatrix},$$

$$\varphi^2(\zeta, u) = \begin{bmatrix} 0 \\ 0 \\ 0 \\ \varphi_4^2(\zeta, u) \end{bmatrix} \quad \text{and} \quad C_2 = \begin{bmatrix} 1 & 0 & 0 & 0 \end{bmatrix},$$

$$A_3(u) = \begin{bmatrix} 0 & 1 \\ 0 & 0 \end{bmatrix},$$

$$\varphi^3(\zeta, u) = \begin{bmatrix} 0 \\ -g + \cos(\theta)\cos(\phi)\dfrac{f}{m} \end{bmatrix} \quad \text{and}$$

$$C_3 = \begin{bmatrix} 1 & 0 \end{bmatrix},$$

$$A_4(u) = \begin{bmatrix} 0 & 1 \\ 0 & 0 \end{bmatrix},$$

$$\varphi^4(\zeta, u) = \begin{bmatrix} 0 \\ a_3\dot{\phi}\dot{\theta} + b_3\tau_\phi \end{bmatrix} \quad \text{and} \quad C_4 = \begin{bmatrix} 1 & 0 \end{bmatrix}.$$

The quadrotor dynamics can be therefore described in the new frame of coordinates as follows

$$\begin{aligned}
\dot{\zeta}(t) &= A\,(u(t))\,\zeta(t) + \varphi\,(u(t), \zeta(t)) \\
\mu(t) &= C\zeta(t),
\end{aligned} \tag{71}$$

where $A(u) = \mathrm{diag}\{A_\kappa(u)\}_{\kappa \in [1,4]}$, $C = \mathrm{diag}\{C_\kappa\}_{\kappa \in [1,4]}$ and $\varphi^T(\zeta, u) = [\varphi^1(u, \zeta) \ \cdots \ \varphi^4(u, \zeta)]$. Moreover, it is worth noticing that the original coordinates can be easily derived from the new coordinates using $\xi = \Phi^{-1}(\zeta)$. This leads to

$$\begin{aligned}
&x = \zeta_1^1, \quad y = \zeta_1^2, \quad z = \zeta_1^3, \quad \theta = \arcsin\left(\zeta_3^1\right), \\
&\phi = \arcsin\left(\frac{-\zeta_3^2}{\cos(\theta)}\right), \quad \psi = \zeta_1^4, \\
&\dot{x} = \zeta_2^1, \quad \dot{y} = \zeta_2^2, \quad \dot{z} = \zeta_2^3, \quad \dot{\theta} = \frac{\zeta_4^1}{\cos(\theta)}, \\
&\dot{\phi} = \frac{\dot{\theta}\sin(\theta)\sin(\phi) - \zeta_4^2}{\cos(\theta)\cos(\phi)}, \quad \dot{\psi} = \zeta_2^4.
\end{aligned} \tag{72}$$

Bearing in mind the fundamental result provided in the last section, it is possible to perform an accurate continuous-time estimation of the position and orientation variables of the quadrotor and their respective translation and angular speeds using only sampled output measurements provided that the involved sampling partition parameter satisfies the requirement (52) and that the considered inputs are persistently exciting according to the assumption **A3**. Such an estimation problem is an adequate opportunity to investigate the feasibility of the proposed observer design framework.

In the following, one shall present a set of simulation results involving a quadrotor model in closed loop with a suitable PD controller with gravity compensation. The involved feedback system is asymptotically stable and able to maintain the vehicle in the desired position with admissible attitude dynamics. The proposed observer has been designed using a quadrotor model which is commonly used in real aerial platforms with $\delta_1 = 5$ and $\delta_2 = \delta_3 = \delta_4 = 1$, according to (7)–(9). The model parameters

are given by

$$m = 0.56Kg, \quad d = 0.21m, \quad I_x = 14.2e^{-3}Kgm^2,$$
$$I_y = 14.2e^{-3}Kgm^2 \quad \text{and} \quad I_z = 2I_x,$$

and the initial conditions for the quadrotor model and the observer have been respectively specified as follows: $\hat{\zeta}(0) = 0.1_{1\times 12}$, $\zeta(0) = 0_{1\times 12}$ and $S_\kappa(0) = I_{12\times 12}$ for $\kappa \in [1, 4]$.

5.1. Continuous observer for a quadrotor

To illustrate the performance of the proposed continuous time observer, some simulations have been carried out. The tuning parameter is setting to $\theta = 1.2$ and a sampling rate 0.005 s. (200 Hz) is considered. Figure 2 shows the evolution of the state, where it is appreciated that the vehicle estimated position converges quickly to real position in less than 5 s, it is also the case of the quadrotor estimate attitude. It is easy to see that the vehicle position and attitude converge to the reference trajectory. This behaviour is that fast thanks to the design of the continuous observer. Notes that the converge is achieved in less that 8 sec.

In order to compare the proposed continuous observer with another works, the simulations have been carried out with the same simulation parameters. Two scenarios are presented with a sampling rate 0.005 s (250 Hz), the first test when the initial conditions for the quadrotor model and the proposed observer are specified as mentioned earlier; and the second test when the initial conditions are set to be zero and, as was considered in Shao et al. (2018). Figure 3 shows the performance of the observer seems similar in both cases, however, this is not presented in Shao et al. (2018), and it was only validated when the initial conditions are set to be zero, this does not allow us to illustrate the convergence of the observation error when tends exponential to zero.

Now, In order to put forward the influence of the increment of the sampling rate on the observation error convergence speed, other values of sampled period Δ_κ have been considered. Indeed,one has compared in Figure 4 the evolutions of the estimation of the positions x and y, the observation error of the position z and the norms of the actual observation error, i.e. $\| \tilde{e} \|$, obtained with three different values of Δ_κ, namely, 0.005, 0.05 and 0.1 s. The obtained results clearly show that the speed of convergence to the state decreases as the sampled period become larger in magnitude reflecting the fact that the typical approach for high gain observer design is inadequate to estimate the state through available measurements

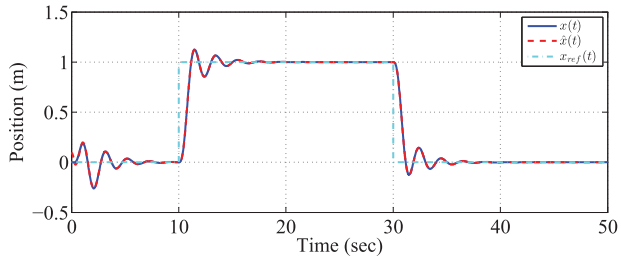

(a) Estimation of the position x

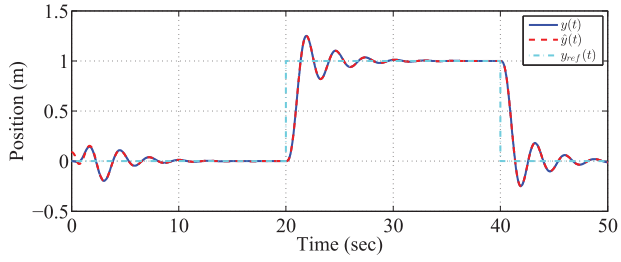

(b) Estimation of the position y

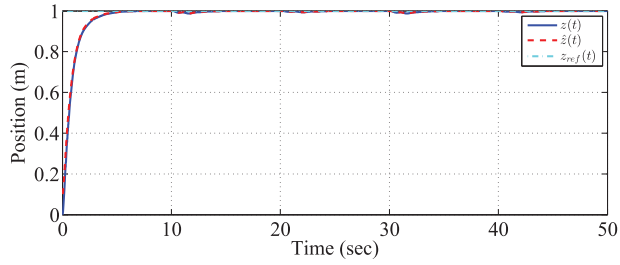

(c) Estimation of the position z

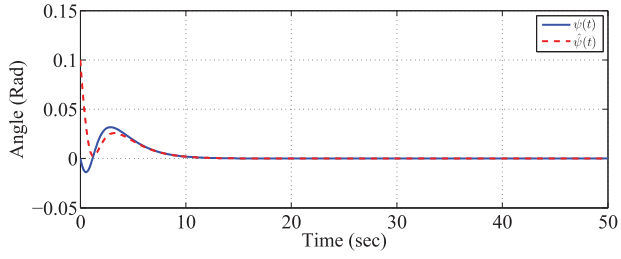

(d) Estimation of the angle ψ

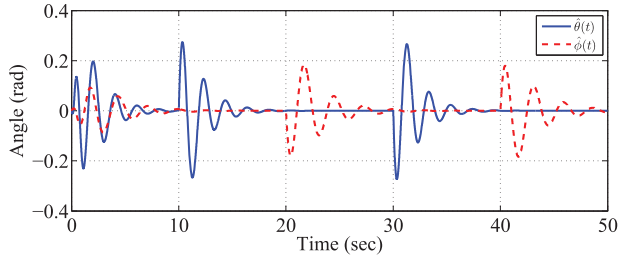

(e) Estimation of the angles θ and ϕ

Figure 2. Estimation of the state UAV in the case continuous with a sampling rate $\Delta_\kappa = 0.005\,s$ (200 Hz).

provided by larger sampled periods. Therefore, there is the need to redesign the typical high gain observer approach.

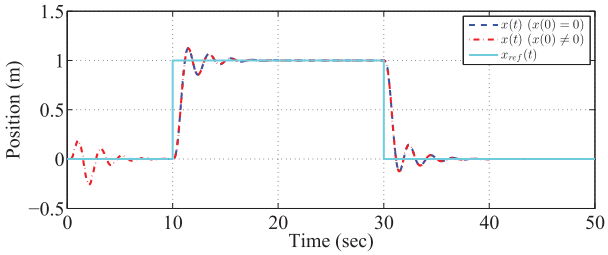

(a) Estimation of the position x

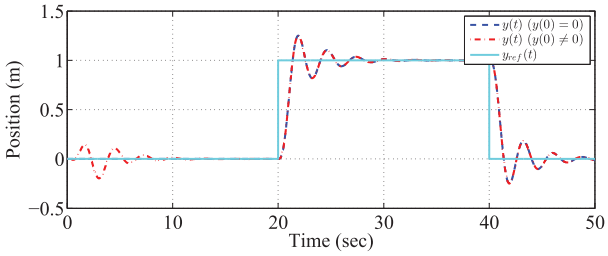

(b) Estimation of the position y

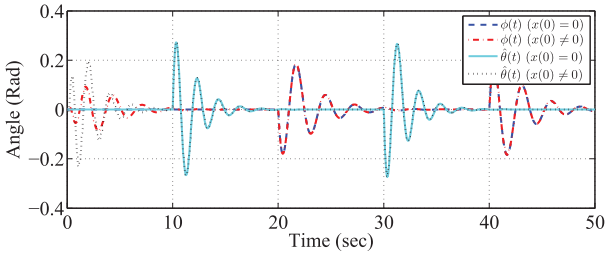

(c) Estimation of the angles θ and ϕ

Figure 3. Evolution of the continuous observer with two different initial conditions by a sampling rate $\Delta_\kappa = 0.004\,s$ (250 Hz).

5.2. Continuous-discrete observer for a quadrotor

To validate the performance of our main contribution which is the continuous-discrete observer, two case studies have been considered depending on the allowed sampling partition bound, namely $\tau_{\min} = 0.05$ s. and $\tau_{\max} = 0.2$ s, allowing thereby to appreciate the observer performance for relatively fast and long sampling processes. The observer design parameter has been specified as follows: $\theta = 1.2$ for low sampling periods and $\theta = 1.15$ for long sampling periods.

Figures 5 and 6 show the state behaviour of the observer for fast and low sampling respectively. It is worth mentioning that the state variables of the quadrotor are accurately estimated. The transient performances are better for the fast sampling case in the considered simulation framework.

Finally, we have compared in Figure 7 two contributions: the continuous observer and the continuous-discrete observer. The results have been obtained by using relatively low sampled periods and long sampled periods, in both observers. It is evident from this results

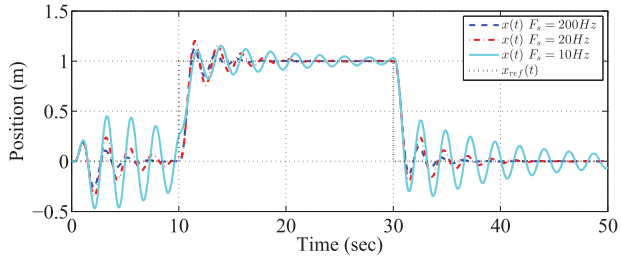

(a) Estimation of the position x

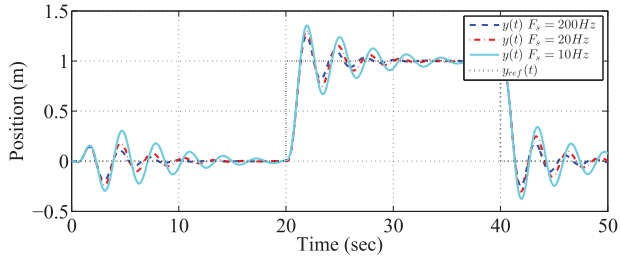

(b) Estimation of the position y

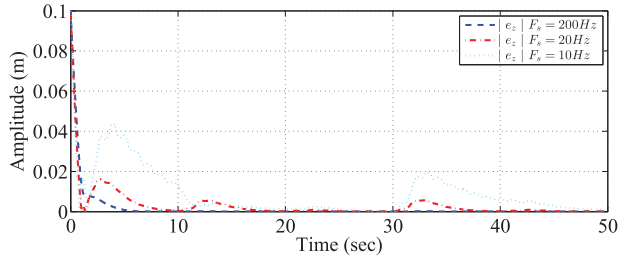

(c) Observation error of the position z | e_z |

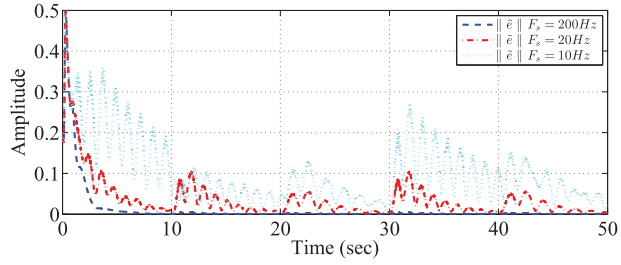

(d) Observation error of the state **UAV** $\|\ \tilde{e}^k\ \|$

Figure 4. Evolution of the continuous observer with different sampling rates $\Delta_\kappa = 0.005$ s, 0.05 s and 0.1 s (200 Hz, 20 Hz and 10 Hz, respectively).

that the speed of convergence to the state decreases as the sampled period become larger in magnitude, however, the continuous-discrete helps to overcome the long sampled periods. This confirms the theoretical results given in Theorem 4.1.

Remark 5.1: It is worth mentioning that the nonlinear systems with coupled structure are usually used in the modelling of quadrotor. In Shao et al. (2018) a structure with strong coupling between position and attitude subsystems is presented, where the available state is $\zeta_1 =$

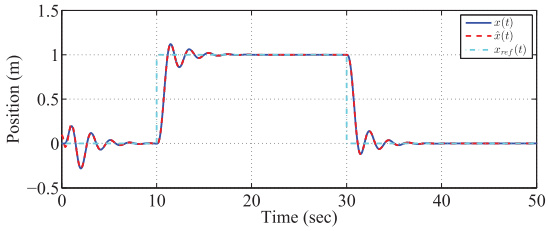

(a) Estimation of the position x

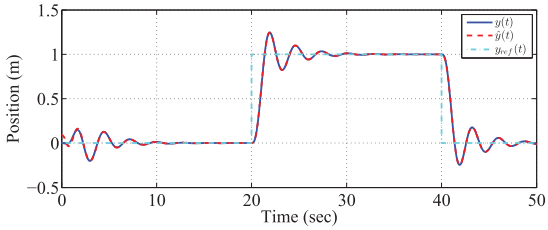

(b) Estimation of the position y

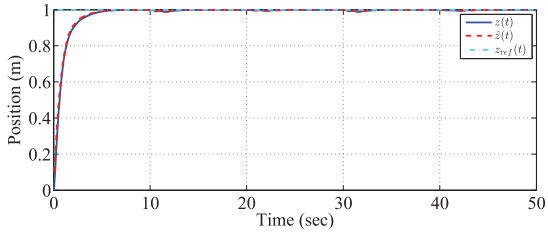

(c) Estimation of the position z

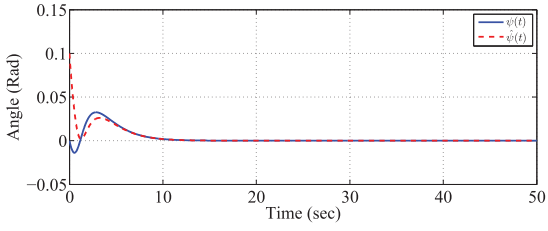

(d) Estimation of the angle ψ

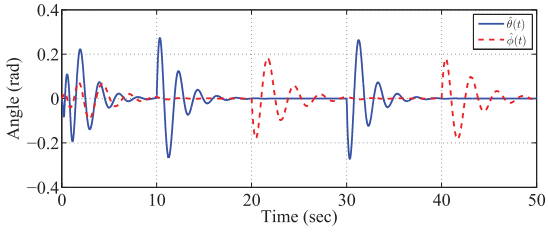

(e) Estimation of the angles θ and ϕ

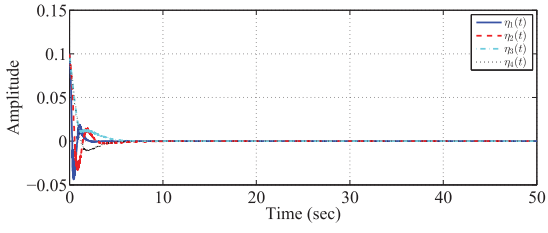

(f) Evolution of the function η_κ

Figure 5. Estimation of the state UAV with sampled period $\Delta_\kappa = 0.05$ s.

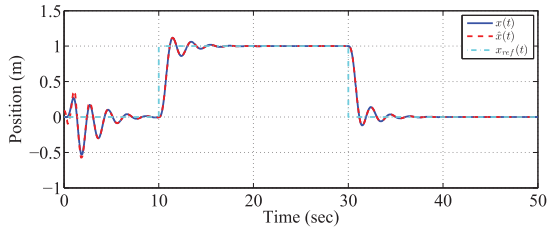

(a) Estimation of the position x

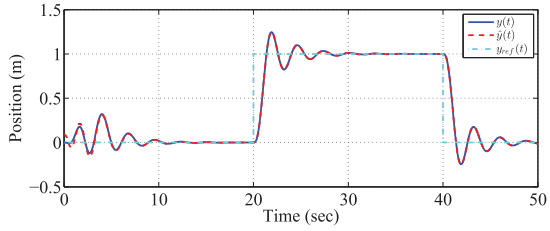

(b) Estimation of the position y

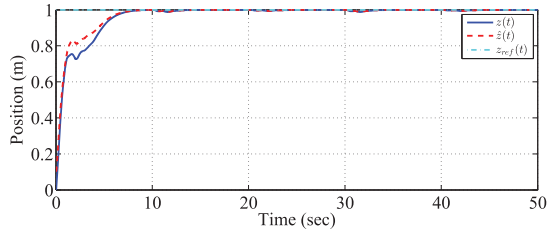

(c) Estimation of the position z

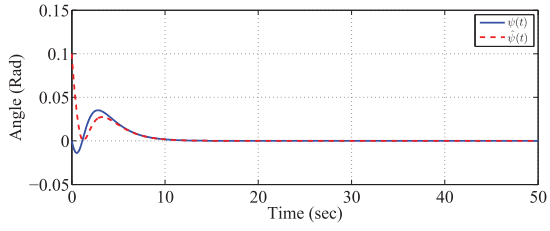

(d) Estimation of the angle ψ

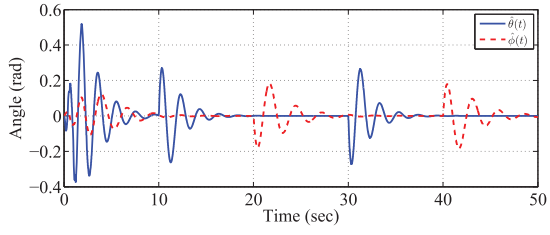

(e) Estimation of the angles θ and ψ

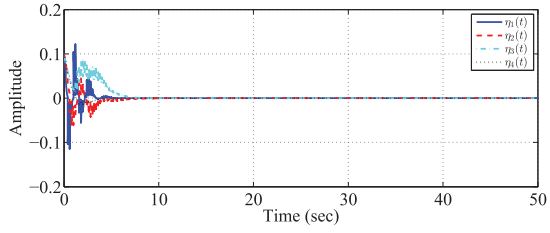

(f) Evolution of the function η_κ

Figure 6. Estimation of the state with sampled period $\Delta_\kappa = 0.2$ s.

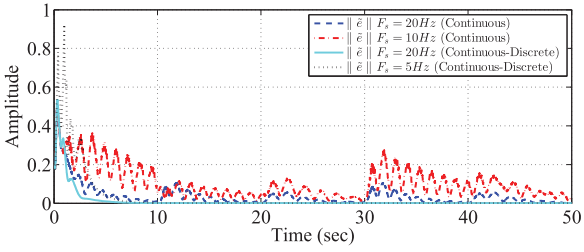

Figure 7. Comparison of the continuous observer and the continuous-discrete observer with different sampling rates.

$[x\ y\ z]$. Another work (Wang et al., 2019), the nonlinear dynamic model of the quadrotor is represented as a integral-chain nonlinear system, where represents two subsystems and the measured state is $\zeta_1 = [z\ \phi\ \theta\ \psi]$. In both cases assume continuous-time measurements when experimental tests, the measurements are available only at sampling instants.

6. Conclusion

We have presented a new high-gain continuous-discrete time observer for a quadrotor. The main contribution of the proposed observer is that it was able to overcome relatively long sampling period. The proposed algorithm has been further validated with simulations for a quadrotor nonlinear model and the results have showed an excellent performance of the proposed scheme. We can appreciate that the behaviour of the continuous-discrete time observer for short sampling times tend to be similar than the behaviour of the continuous time observer. However, in the case of long sampling times the performances are still very good. In our future research we intend to consider a varying sampling time. It would also be interesting to obtain experimental results.

Disclosure statement

No potential conflict of interest was reported by the authors.

Notes on contributors

Omar Hernández-González received his M.Sc. degree in electronic engineering from CENIDET, México, in 2008, and the Ph.D. degree in automatic control from the University of Caen Normandie, France, in 2017. Since 2008, he has held a position of Professor in the Technological Institute of México/Coatzacoalcos (ITESCO). His research interests include the nonlinear observers, nonlinear control, and UAV.

María-Eusebia Guerrero-Sánchez María-Eusebia Guerrero-Sánchez received the Ph.D. degree in electronic engineering from the Centro Nacional de Investigación y Desarrollo Tecnológico (CENIDET), México, in 2017. She is currently a Professor at the Technological Institute of México/Coatzacoalcos (ITESCO). Her research interests are focused on passivity-based control, nonlinear control, and UAV.

Mondher Farza received his degrees of engineering and M.Sc. in computer sciences and applied mathematics from ENSEEIHT Toulouse in 1988. Then, he joined the Laboratoire d'Automatique de Grenoble from 1988 to 1994 and obtained his Ph.D. in control sciences in 1992. From 1994 to 1997, he occupied a postdoctoral position at Laboraoire d'Automatique et de Génie de Procédés in Lyon. He joined the University of Caen Normandie in 1997 where he occupies since 2007 the position of Professor. His research interests are in nonlinear control and systems and applications.

Tomas Ménard received the B.S. and M.S. degrees in Mathematics from the University of Nantes, France, in 2005 and 2008, respectively. He joined the IRCCyN laboratory at Ecole Centrale de Nantes in 2008, where he received the Ph.D. degree in 2011. From 2011 to 2012, he held a postdoctoral position at the Research Center 'E. Piaggio' of the University of Pisa. In 2012, he joined the University of Caen, where he is currently assistant-professor. He received his Habilitation to direct research in 2017. In 2017–2018 he was teacher at Rajamangala University of Technology Thanyaburi, Thailand. His research interests include nonlinear observers, homogeneity theory and identification.

Mohammed M'Saad was educated at the Ecole Mohammadia d'Ingénieurs where he held an assistant professor position in September 1978. He started his research activities at the LEESA where he prepared an engineering thesis of the Université de Mohammed V on the adaptive control of industrial processes. In November 1982, Mohammed M'SAAD joined the LAG to prepare a Ph.D. thesis of the Institut National Polytechnique de Grenoble on the fundamental features of the adaptive control and its applicability, which he obtained in April 1987. In April 1988, he held a research position at the CNRS with an affectation in the LAG. In September 1996, Mohammed M'Saad held a professor position at the ENSICAEN where he founded a control process laboratory in 1997 which became a control group at the GREYC UMR CNRS in January 2004 and a Control Laboratory of Caen since March 2017. His main research activities are mainly devoted to the fundamental, methodological and applied features of the identification, observation and adaptive control of dynamical systems.

Rogelio Lozano is CNRS Research Director at UTC, France. He obtained his Ph.D. degree in automatic control at Laboratoire d'Automatique de Grenoble, INPG in 1981. He was Professor at CINVESTAV, Mexico 1981–1989. He was a visiting professor at the University of Newcastle, Australia 1984–1985. He was Senior Researcher at NASA Langley Research Center, USA, 1987–1988. He was Head of the Heudiasyc Lab from 1995 to 2007. He was Associate Editor of Automatica from 1987 to 2000. He was member of the French National Committee from 2000 to 2006. He was Head of International Collaborations at CNRS STIC Department from 2006 to 2009. Since 2008 he is Head of the Joint Mexican-French UMI 3175 CNRS. He is currently associate Editor of the *Journal of Intelligent and Robotics Systems* since 2012 and Associate Editor in the *International Journal of Adaptive Control and Signal Processing* since 1988.

References

Arcak, M., & Nesic, D. (2004). A framework for nonlinear sampled-data observer design via approximate discrete-time models and emulation. *Automatica*, *40*, 1931–1938.

Besançon, G., Bornard, G., & Hammouri, H. (1996). Observer synthesis for a class of nonlinear control systems. *European Journal of Control*, *2*(3), 176–192.

Besançon, G., & Ticlea, A. (2007). An immersion-based observer design for rank-observable nonlinear systems. *IEEE Transactions on Automatic Control*, *52*(1), 83–88.

Bouraoui, I., Farza, M., Ménard, T., Abdennour, R. B., M'Saad, M., & Mosrati, H. (2015). Observer design for a class of uncertain nonlinear systems with sampled outputs: Application to the estimation of kinetic rates in bioreactors. *Automatica*, *55*, 78–87.

Busawon, K., Farza, M., & Hammouri, H. (1998). A nonlinear observer for induction motors. *International Journal of Control*, *71*, 405–418.

Castañeda, H., Salas-Peña, O.-S., & de Leon-Morales, J. (2017). Extended observer based on adaptive second order sliding mode control for a fixed wing uav. *ISA Transactions*, *66*, 226–232.

Castillo, A., Sanz, R., Garcia, P., Qiu, W., Wang, H., & Xu, C. (2019). Disturbance observer-based quadrotor attitude tracking control for aggressive maneuvers. *Control Engineering Practice*, *82*, 14–23.

Deza, F., Busvelle, E., & Gauthier, J. (1992). Exponentially converging observers for distillation columns and internal stability of the dynamic output feedback. *Chemical Engineering Science*, *47*(15–16), 3935–3941.

Deza, F., Busvelle, E., Gauthier, J., & Rakotopara, D. (1992). High gain estimation for nonlinear systems. *Systems & Control Letters*, *18*(4), 295–299.

Dinh, T. N., Andrieu, V., Nadri, M., & Serres, U. (2015). Continuous-discrete time observer design for lipschitz systems with sampled measurements. *IEEE Transactions on Automatic Control*, *60*(3), 787–792.

Dufour, P., Flila, S., & Hammouri, H. (2012). Observer design for mimo non-uniformly observable systems. *IEEE Transactions on Automatic Control*, *57*, 511–516.

Farza, M., Bouraoui, I., Ménard, T., Abdennour, R. B., & M'Saad, M. (2014). Adaptive observers for a class of uniformly observable systems with nonlinear parametrization and sampled outputs. *Automatica*, *50*, 2951–2960.

Farza, M., M'Saad, M., Fall, M., Pigeon, E., Gehan, O., & Busawon, K. (2014). Continuous-discrete time observers for a class of mimo nonlinear systems. *IEEE Transactions on Automatic Control*, *59*, 1060–1065.

Farza, M., M'Saad, M., & Rossignol, L. (2004). Observer design for a class of mimmo nonlinear systems. *Automatica*, *40*, 135–143.

Farza, M., Triki, M., M'Saad, M., & Maatoug, T. (2011). High gain observer for a class of non-triangular systems. *Systems & Control Letters*, *60*(1), 27–35.

Gauthier, J., Hammouri, H., & Othman, S. (1992). A simple observer for nonlinear systems. Applications to bioreactors. *IEEE Transactions on Automatic Control*, *37*(6), 875–880.

Gauthier, J., & Kupka, I. (2001). *Deterministic observation theory and applications*. Cambridge: Cambridge University Press.

Guisser, M., & Medromi, H. (2009). A high gain observer and sliding mode controller for an autonomous quadrotor helicopter. *International Journal of Intelligent Control and Systems*, *14*(3), 204–212.

Hammouri, H., Bornard, G., & Busawon, K. (2010). High gain observer for structured multi-output nonlinear systems. *IEEE Transactions on Automatic Control*, *55*, 987–992.

Hammouri, H., & Farza, M. (2003). Nonlinear observers for locally uniformly observable systems. *ESAIM: Control, Optimisation and Calculus of Variations*, *9*, 353–370.

Hammouri, H., Nadri, M., & Mota, R. (2006). *Constant gain observer for continuous-discrete time uniformly observable systems*. 45th IEEE Conference on Decision and Control (CDC), San Diego, CA (pp. 5406–5411).

Hernández-González, O., Farza, M., Ménard, T., Targui, B., M'Saad, M., & Astorga-Zaragoza, C.-M. (2016). A cascade observer for a class of mimo non uniformly observable systems with delayed sampled outputs. *Systems & Control Letters*, *98*, 86–96.

Hou, M., Busawon, K., & Saif, M. (2000). Observer design for a class of MIMO nonlinear systems. *IEEE Transactions on Automatic Control*, *45*(7), 1350–1355.

Karafyllis, I., & Kravaris, C. (2009). From continuous-time design to sampled-data design of observers. *IEEE Transactions on Automatic Control*, *54*(9), 2169–2174.

Krener, N., & Kravaris, C. (2001). Discrete-time nonlinear observer design using functional equations. *Systems & Control Letters*, *42*, 81–94.

Nadri, M., Hammouri, H., & Astorga, C. (2004). Observer design for continuous-discrete time state affine systems up to output injection. *European Journal of Control*, *10*, 252–263.

Rosaldo-Serrano, M. A., Santiaguillo-Salinas, J., & Aranda-Bricaire, E. (2019). Observer-based time-varying backstepping control for a quadrotor multi-agent system. *Journal of Intelligent & Robotic Systems*, *93*, 135–150.

Shao, X., Liu, J., & Wang, H. (2018). Robust back-stepping output feedback trajectory tracking for quadrotors via extended state observer and sigmoid tracking differentiator. *Mechanical Systems and Signal Processing*, *104*, 631–647.

Shim, H., Son, Y., & Seo, J. (2001). Semi-global observer for multi-output nonlinear systems. *Systems & Control Letters*, *42*(3), 233–244.

Wang, B., Yu, X., Mu, L., & Zhang, Y. (2019). Disturbance observer-based adaptive fault-tolerant control for a quadrotor helicopter subject to parametric uncertainties and external disturbances. *Mechanical Systems and Signal Processing*, *120*, 727–743.

Zhao, G., & Hua, C. (2017). Continuous-discrete-time adaptive observers for nonlinear systems with sampled output measurements. *International Journal of Systems Science*, *48*(12), 2599–2609.

Zhao, G., & Wang, J. (2014). Reset observers for linear time-varying delay systems: Delay-dependent approach. *Journal of the Franklin Institute*, *351*(11), 5133–5147.